



7-2017

Equine Arteritis Virus Has Specific Tropism for Stromal Cells and CD8⁺ T and CD21⁺ B Lymphocytes but Not for Glandular Epithelium at the Primary Site of Persistent Infection in the Stallion Reproductive Tract

Mariano Carossino

University of Kentucky, mcarossino@uky.edu

Alan T. Loynachan

University of Kentucky, alan.loynachan@uky.edu

Igor F. Canisso

University of Illinois at Urbana-Champaign

Richard Frank Cook

University of Kentucky, richard.cook@uky.edu

Juliana Roberta Campos

University of Kentucky, jrcampos_unesp@yahoo.com.br

Repository Citation


Carossino, Mariano; Loynachan, Alan T.; Canisso, Igor F.; Cook, Richard Frank; Campos, Juliana Roberta; Nam, Bora; Go, Yun Young; Squires, Edward L.; Troedsson, Mats H. T.; Swerczek, Thomas W.; Del Piero, Fabio; Bailey, Ernest F.; Timoney, Peter J.; and Balasuriya, Udeni B. R., "Equine Arteritis Virus Has Specific Tropism for Stromal Cells and CD8⁺ T and CD21⁺ B Lymphocytes but Not for Glandular Epithelium at the Primary Site of Persistent Infection in the Stallion Reproductive Tract" (2017). *Veterinary Science Faculty Publications*. 39.

https://uknowledge.uky.edu/gluck_facpub/39

See next page for additional authors

Right click to open a feedback form in a new tab to let us know how this document benefits you.

Follow this and additional works at: https://uknowledge.uky.edu/gluck_facpub

 Part of the [Large or Food Animal and Equine Medicine Commons](#), [Veterinary Infectious Diseases Commons](#), [Veterinary Microbiology and Immunobiology Commons](#), and the [Veterinary Physiology Commons](#)

Authors

Mariano Carossino, Alan T. Loynachan, Igor F. Canisso, Richard Frank Cook, Juliana Roberta Campos, Bora Nam, Yun Young Go, Edward L. Squires, Mats H. T. Troedsson, Thomas W. Swerczek, Fabio Del Piero, Ernest F. Bailey, Peter J. Timoney, and Udeni B. R. Balasuriya

Equine Arteritis Virus Has Specific Tropism for Stromal Cells and CD8⁺ T and CD21⁺ B Lymphocytes but Not for Glandular Epithelium at the Primary Site of Persistent Infection in the Stallion Reproductive Tract**Notes/Citation Information**

Published in *Journal of Virology*, v. 91, issue 13, e00418-17, p. 1-26.

Copyright © 2017 American Society for Microbiology. All Rights Reserved.

The copyright holder has granted the permission for posting the article here.

Digital Object Identifier (DOI)

<https://doi.org/10.1128/JVI.00418-17>



Equine Arteritis Virus Has Specific Tropism for Stromal Cells and CD8⁺ T and CD21⁺ B Lymphocytes but Not for Glandular Epithelium at the Primary Site of Persistent Infection in the Stallion Reproductive Tract

Mariano Carossino,^a Alan T. Loynachan,^b Igor F. Canisso,^c R. Frank Cook,^a Juliana R. Campos,^a Bora Nam,^a Yun Young Go,^{a,d} Edward L. Squires,^a Mats H. T. Troedsson,^a Thomas Swerczek,^a Fabio Del Piero,^e Ernest Bailey,^a Peter J. Timoney,^a Udeni B. R. Balasuriya^a

Department of Veterinary Science, Maxwell H. Gluck Equine Research Center, College of Agriculture, Food and Environment, University of Kentucky, Lexington, Kentucky, USA^a; University of Kentucky Veterinary Diagnostic Laboratory, College of Agriculture, Food and Environment, University of Kentucky, Lexington, Kentucky, USA^b; Department of Veterinary Clinical Medicine and Department of Comparative Biosciences, College of Veterinary Medicine, University of Illinois Urbana-Champaign, Urbana, Illinois, USA^c; Virus Research and Testing Group, Division of Drug Discovery Research, Korea Research Institute of Chemical Technology, Yuseong-gu, Daejeon, South Korea^d; Department of Pathobiological Sciences, School of Veterinary Medicine, Louisiana State University, Baton Rouge, Louisiana, USA^e

ABSTRACT Equine arteritis virus (EAV) has a global impact on the equine industry as the causative agent of equine viral arteritis (EVA), a respiratory, systemic, and reproductive disease of equids. A distinctive feature of EAV infection is that it establishes long-term persistent infection in 10 to 70% of infected stallions (carriers). In these stallions, EAV is detectable only in the reproductive tract, and viral persistence occurs despite the presence of high serum neutralizing antibody titers. Carrier stallions constitute the natural reservoir of the virus as they continuously shed EAV in their semen. Although the accessory sex glands have been implicated as the primary sites of EAV persistence, the viral host cell tropism and whether viral replication in carrier stallions occurs in the presence or absence of host inflammatory responses remain unknown. In this study, dual immunohistochemical and immunofluorescence techniques were employed to unequivocally demonstrate that the ampulla is the main EAV tissue reservoir rather than immunologically privileged tissues (i.e., testes). Furthermore, we demonstrate that EAV has specific tropism for stromal cells (fibrocytes and possibly tissue macrophages) and CD8⁺ T and CD21⁺ B lymphocytes but not glandular epithelium. Persistent EAV infection is associated with moderate, multifocal lymphoplasmacytic ampullitis comprising clusters of B (CD21⁺) lymphocytes and significant infiltration of T (CD3⁺, CD4⁺, CD8⁺, and CD25⁺) lymphocytes, tissue macrophages, and dendritic cells (Iba-1⁺ and CD83⁺), with a small number of tissue macrophages expressing CD163 and CD204 scavenger receptors. This study suggests that EAV employs complex immune evasion mechanisms that warrant further investigation.

IMPORTANCE The major challenge for the worldwide control of EAV is that this virus has the distinctive ability to establish persistent infection in the stallion's reproductive tract as a mechanism to ensure its maintenance in equid populations. Therefore, the precise identification of tissue and cellular tropism of EAV is critical for understanding the molecular basis of viral persistence and for development of im-

Received 13 March 2017 Accepted 11 April 2017

Accepted manuscript posted online 19 April 2017

Citation Carossino M, Loynachan AT, Canisso IF, Cook RF, Campos JR, Nam B, Go YY, Squires EL, Troedsson MHT, Swerczek T, Del Piero F, Bailey E, Timoney PJ, Balasuriya UBR. 2017. Equine arteritis virus has specific tropism for stromal cells and CD8⁺ T and CD21⁺ B lymphocytes but not for glandular epithelium at the primary site of persistent infection in the stallion reproductive tract. *J Virol* 91:e00418-17. <https://doi.org/10.1128/JVI.00418-17>.

Editor Stanley Perlman, University of Iowa

Copyright © 2017 American Society for Microbiology. All Rights Reserved.

Address correspondence to Udeni B. R. Balasuriya, ubalasuriya@uky.edu.

proved prophylactic or treatment strategies. This study significantly enhances our understanding of the EAV carrier state in stallions by unequivocally identifying the ampullae as the primary sites of viral persistence, combined with the fact that persistence involves continuous viral replication in fibrocytes (possibly including tissue macrophages) and T and B lymphocytes in the presence of detectable inflammatory responses, suggesting the involvement of complex viral mechanisms of immune evasion. Therefore, EAV persistence provides a powerful new natural animal model to study RNA virus persistence in the male reproductive tract.

KEYWORDS arterivirus, equine arteritis virus, EAV, equine viral arteritis, EVA, persistent infection, male reproductive tract, immunohistochemistry, cellular tropism, immune response

Equine arteritis virus (EAV), the prototype member of the family *Arteriviridae*, genus *Arterivirus*, in the order *Nidovirales* (1), is the causative agent of equine viral arteritis (EVA), a respiratory, systemic, and reproductive disease of equids. EAV has a worldwide distribution, and it causes significant economic loss to the equine industry in the United States and other countries (2–8). EAV contains a positive-sense, single-stranded RNA genome (~12.7 kb) containing 10 known open reading frames (ORFs) (2, 3, 9, 10). ORFs 1a and 1b encode two replicase polyproteins (pp1a and pp1ab) that are cleaved to give rise to 13 nonstructural proteins (nsp1 to nsp12 and nsp7 α /nsp7 β), whereas ORFs 2a, 2b, 3, 4, 5a, 5b, 6, and 7 encode the viral structural proteins E, GP2, GP3, GP4, ORF5a protein, GP5, M, and N (nucleocapsid protein), respectively (3, 9, 10).

Following respiratory or venereal exposure, EAV induces a cell-associated viremia and a systemic panvasculitis involving small muscular arteries (2, 3, 11–17). Acutely infected horses may develop a wide range of clinical signs (influenza-like syndrome), with dependent edema, conjunctivitis, periorbital or supraorbital edema, respiratory distress, urticaria, and leukopenia (2–4, 8, 15, 17–23). However, a remarkable property of EAV is that following initial exposure, it can establish persistent infection in the reproductive tract of stallions, resulting in continuous shedding of infectious virus in semen (2–4). Although in some cases this ceases at only a few weeks or a few months postinfection, in 10 to 70% of infected stallions shedding can continue for many years or even the remainder of the animal's lifetime (2–4, 18, 24–27). Interestingly, EAV carriers do not exhibit clinical disease, and reproductive fecundity is not decreased (8, 24, 25). Furthermore, EAV is detectable only in the reproductive tract of these stallions, and the virus persists despite the presence of neutralizing antibodies in serum (2–4, 8, 18, 24, 25, 27, 28). Persistently infected stallions play a major epidemiological role since they constitute the natural reservoir for EAV and, thus, are responsible for the maintenance and perpetuation of EAV in equine populations between breeding seasons (2–4, 18, 27). Viral evolution and emergence of novel genetic and antigenic variants are associated with long-term persistent infection in the reproductive tract of the stallion (3, 26, 29–31), and the maintenance of the carrier state is androgen dependent (8), as evidenced by the fact that the only documented method to prevent viral shedding in long-term carrier stallions is surgical castration (32).

Many different viruses can establish relatively long-term or even persistent infections in the mammalian male reproductive tract despite the resolution of clinical signs and establishment of adaptive immune responses (33). Indeed, it has been recently shown that Zika virus can be shed in semen for periods up to 80 days, with viral nucleic acids detectable for as long as 6 months following infection (34–38). Unfortunately, the mechanisms by which such infections are maintained have not been extensively investigated in most cases despite the fact that they may represent a major mode of transmission within mammalian populations. However, we recently reported that EAV carrier status in stallions correlates with possession of a subpopulation of CD3⁺ T lymphocytes that is susceptible to viral infection *in vitro* (39, 40). On the other hand, stallions that lack this subpopulation are at significantly lower risk of becoming persistently infected (39). Furthermore, a genome-wide association study (GWAS) con-

TABLE 1 Stallions included in the study ($n = 13$)

Stallion identification	Infection status at time of euthanasia	Duration of viral shedding (dpi) ^a	Viral titer in semen (PFU/ml) ^b
N105	Control	NA	NA
N121	Control	NA	NA
O103	Control	NA	NA
O113	Control	NA	NA
L136	Persistently infected	≥ 726	6.5×10^3
L140	Persistently infected	≥ 726	7.8×10^3
Stallion E	Persistently infected	~ 7 yr	1×10^5
L137	Stopped shedding	149	0
L138	Stopped shedding	128	0
L139	Stopped shedding	380	0
L141	Stopped shedding	380	0
L142	Stopped shedding	198	0
L143	Stopped shedding	ND	ND

^aExcept as noted, values represent days postinfection (dpi). NA, not applicable; ND, not determined.

^bViral titers in semen correspond to ejaculates obtained by 726 dpi with the exception of that of stallion E.

ducted by this laboratory revealed that the ability of EAV to infect CD3⁺ T lymphocytes and establish long-term carrier status in stallions is strongly associated with four nucleotide changes in the CXCL16 gene located on equine chromosome 11 (41, 42). To our knowledge this is the first demonstration of a correlation between a viral carrier state and a host genetic component. As such, it adds impetus to the study of EAV persistence in the stallion reproductive system as a model of viral persistence in the mammalian male reproductive tract. Continuation of this work, however, necessitates identification of the sites of viral persistence within the stallion reproductive tract and, just as importantly, the host cell types that are capable of supporting EAV replication. An additional consideration is to determine if EAV replication in persistently infected stallions triggers active immunological responses. Although a previous study suggested that EAV could be primarily isolated from an accessory sex gland, the ampulla, the experiments were conducted exclusively using homogenized tissue samples (43) and, therefore, were of little value in terms of identifying either EAV host cell tropism within the stallion's reproductive tract tissues or detecting the presence of inflammatory responses. In addition, the methodologies employed in the previous study make it impossible to determine if the ampulla is the primary site of active EAV replication or if viral particles simply accumulate in this accessory sex gland. However, on the basis of virus isolation, we hypothesized that EAV persists in non-immunologically privileged tissues of the stallion's genital tract and that viral replication within specific cell types at these sites is associated with modulation of immunological responses that prevent excessive tissue damage resulting in gross pathological lesions. In this study, we have combined virus isolation, insulated isothermal reverse transcription-PCR (RT-iiPCR), single and dual immunohistochemistry (IHC), immunofluorescent antibody (IFA), and transmission electronic microscopy (TEM) techniques to unequivocally demonstrate EAV tissue and cellular localization in the stallion reproductive tract during persistent infection. Our findings provide compelling evidence that persistent EAV infection is associated with certain subpopulations of infiltrating T and B lymphocytes and of stromal cells (fibrocytes and possibly tissue macrophages), with a specific homing to the accessory sex glands despite the strong humoral and local inflammatory response of the host. Consequently, the stallion accessory sex glands must represent a highly specialized microenvironment that enable EAV persistence, making this system a powerful natural animal model for studying host-RNA virus interactions in the mammalian male reproductive tract.

RESULTS

Clinical outcome and establishment of EAV persistent infection in experimentally infected stallions. All experimentally infected stallions ($n = 8$) (Table 1) developed moderate to severe clinical signs of EVA following intranasal infection with the

TABLE 2 Median duration and peak of clinical signs after experimental infection with the EAV KY84 strain ($n = 8$)

Clinical sign	Median duration (days [IQR])	Median peak (dpi)
Hyperthermia ^a	6 (2)	6.5
Edema	20 (14.25)	9.25
Nasal discharge	3 (6)	6.5
Congestion or hemorrhage of oral mucosa	2 (1.5)	6.5
Leukopenia	8 (15)	8

^aHyperthermia was considered to be a body temperature of $\geq 38.6^{\circ}\text{C}$.

EAV KY84 strain. Clinical signs started at 2 days postinfection (dpi) and included fever (38.7°C to 40.8°C [101.7°F to 105.6°F]), leukopenia, edema in multiple locations (ocular, scrotal, preputial, and limb edema), nasal and ocular discharge, photophobia, anorexia, decreased libido, and congestion and petechial or ecchymotic hemorrhages on the oral mucosal membranes (Table 2). Clinical signs lasted for a median of 20 days (interquartile range [IQR], 11.25 days; range, 10 to 28 days), and their peak occurred at a median of 7 dpi (Fig. 1). No signs of disease were observed after clinical recovery and until the conclusion of the experimental study. Viral shedding in nasal secretions was detected as early as 2 dpi, with a median duration of 10 days (IQR, 2 days; range, 8 to 19 days) and a mean viral titer of 4.36×10^3 PFU/ml (range, ≤ 10 to 5.7×10^4 PFU/ml). Similarly, viremia was detected in buffy coat cells at 2 dpi but was extended to between 28 and 42 dpi, with a median duration of 26 days (IQR, 17.5 days; range, 12 to 40 days) and a mean viral infectivity titer of 2.35×10^2 PFU/ml (range, ≤ 10 to 5.1×10^3 PFU/ml) (Fig. 1). The peak for both nasal shedding and viremia occurred at a median of 6 dpi. The clearance of virus from blood mononuclear cells coincided with the appearance of neutralizing antibodies. All stallions seroconverted starting from 8 dpi and maintained high serum neutralizing antibody titers until the end of the study (1:64 to $>1:512$; median titer, 1:256) (data not shown). Viral shedding in semen started at 5 dpi, except for in one stallion (L141), where it was detected at 3 dpi. Viral infectivity titers in semen varied from 1.0×10^1 to 1.88×10^7 PFU/ml during the acute phase of infection (up to 21 dpi), with a mean titer of 7.85×10^5 PFU/ml. A peak in viral infectivity titers in semen occurred at a median of 9 dpi.

All experimentally infected stallions showed decreased libido during the acute phase of infection. However, neither clinical signs of EVA nor reproductive dysfunction were observed in any of the experimentally infected stallions ($n = 8$) (Table 1) at the time of euthanasia. Two out of 8 experimentally infected stallions (L136 and L140)

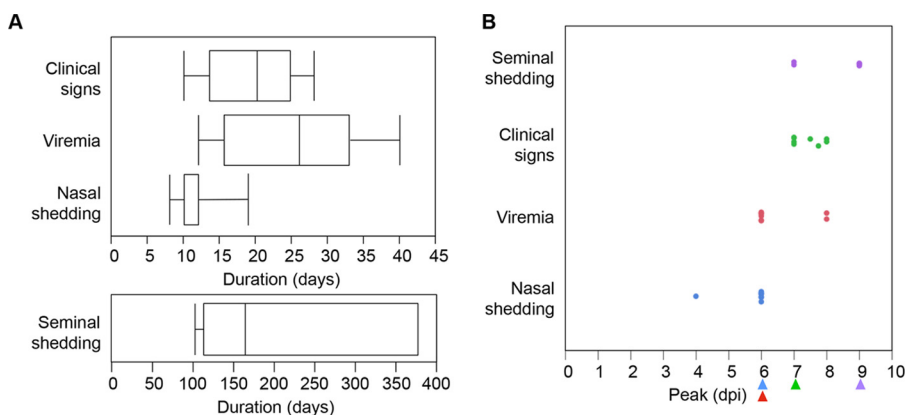


FIG 1 Clinical outcome following experimental infection of stallions with EAV KY84 strain ($n = 8$). Duration (in days) (A) and peak (dpi) (B) of nasal shedding, viremia, clinical signs, and seminal shedding. The data shown for seminal shedding in panel A correspond to the experimentally infected stallions that stopped shedding virus in semen during the course of the study ($n = 6$). Median peaks are marked with an arrowhead, and dots represent individual stallions.

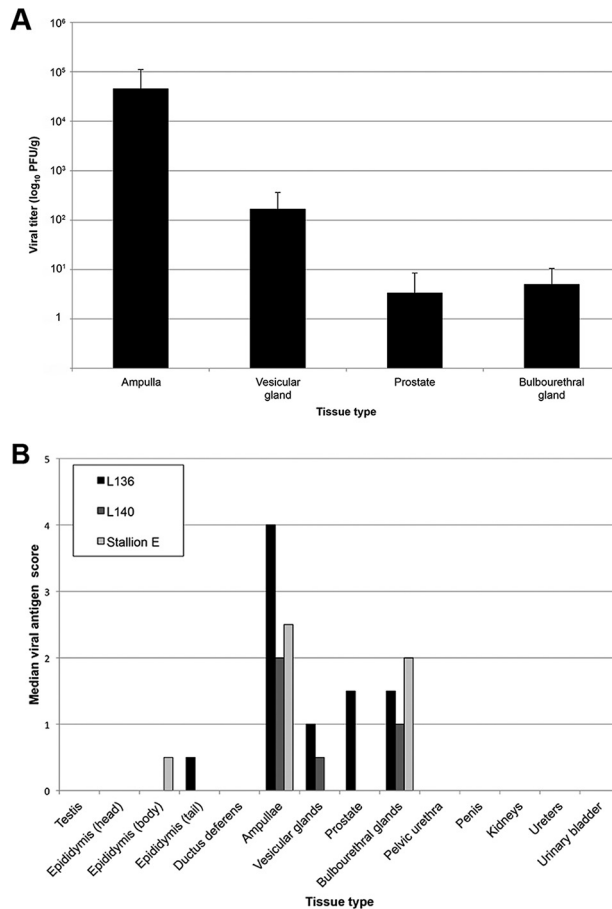


FIG 2 Viral infectivity titers and viral antigen scores per tissue type derived from EAV long-term persistently infected stallions ($n = 3$). (A) Mean viral infectivity titers in long-term persistently infected stallions per tissue type. Bars represent the standard deviations. (B) Median viral antigen scores from long-term persistently infected stallions per tissue type. Viral antigen in tissues was detected using an EAV N protein-specific monoclonal antibody (3E2) and a Bond Polymer Refine Red Detection kit. 0, negative; 1, <5 positive cells; 2, 5 to ≤ 45 positive cells; 3, 46 to ≤ 125 positive cells; 4, 126 to ≤ 250 positive cells; 5, >250 positive cells. Scores reflect the cumulative number of positive cells in five $\times 100$ (total magnification) fields.

continued to shed EAV in their semen for ≥ 726 dpi (i.e., long-term persistently infected stallions). By the end of the study, viral titers in their semen were 6.5×10^3 and 7.8×10^3 PFU/ml, respectively (Table 1), but infectivity titers in these stallions fluctuated from 1.2×10^3 to 8.8×10^5 PFU/ml after resolution of clinical signs. The remaining stallions shed virus in their semen for a variable period of time after experimental infection, with a range of 128 to 380 dpi and a median duration of EAV seminal shedding of 165 days (IQR, 263.5 days; range, 102 to 377 days) (Table 1 and Fig. 1). For behavioral reasons, semen collection from one of the stallions (L143) was not feasible, and the carrier status could not be determined until the end of the study. Stallion E (naturally infected) had shed EAV in semen for approximately 7 years, with a mean titer of 1.0×10^5 PFU/ml, with no clinical signs of EVA or reproductive dysfunction. None of the stallions were viremic or shed EAV in nasal secretions at the time of euthanasia.

Identification of EAV main tissue reservoirs during persistent infection in the reproductive tract of the stallion. EAV was isolated from several tissues of the reproductive tract of long-term persistently infected stallions ($n = 3$; L136, L140, and stallion E) with marked variation in viral titers among tissues (range, <10 to 1.7×10^5 PFU/g). EAV was isolated from the ampullae in all cases and presented the highest viral infectivity titers of the tissues examined (mean viral titer of 4.52×10^4 PFU/g; range, 1.0×10^3 to 1.7×10^5 PFU/g) (Fig. 2A). Infectious virus could be recovered from either

one or both vesicular glands in persistently infected stallions, but infectivity titers were approximately 100-fold lower than those observed in the ampullae (mean viral titer of 1.67×10^2 PFU/g; range, 1.0×10^2 to 5.0×10^2 PFU/g). EAV was recovered from the prostate gland of a single persistently infected stallion (stallion E) and from one or both bulbourethral glands in all of them. However, mean viral titers for both of these accessory sex glands were very low (<10 PFU/g) (Fig. 2A). In addition, EAV was isolated from the tail of the left epididymis (1.0×10^2 PFU/g) and the left ductus deferens (mean viral titer of 3.5×10^3 PFU/g) of a single persistently infected stallion (stallion E). Regional lymph nodes associated with the reproductive tract (superficial and deep inguinal, lumbar, and iliac lymph nodes), other lymphoid tissues (e.g., spleen, splenic lymph node, and bone marrow), and other body tissues from three long-term persistently infected stallions failed to yield virus following two blind passages in cell culture. Similarly, virus was not isolated from any body tissues, including the reproductive tract, of the stallions that stopped shedding virus in their semen during the course of the study (stallions L137, L138, L139, L141, L142, and L143).

Single immunohistochemistry (IHC) and immunofluorescent antibody (IFA) staining for the detection of EAV antigen were used to quantify EAV-positive cells in tissues from the reproductive tract of persistently infected stallions. Immunostaining demonstrated the presence of intracytoplasmic antigen predominantly localized in stromal cells (spindle-shaped cells, consistent with fibrocytes) and lymphocytes that were either present within inflammatory infiltrates or scattered through the lamina propria of the ampullae and, rarely, in the interstitium of the epididymides and other accessory sex glands (vesicular glands, prostate, and bulbourethral glands) (Fig. 3). EAV antigen-positive subepithelial and intraepithelial lymphocytes were observed in close association with and across the glandular epithelium of the ampullae (Fig. 3), and some EAV-positive cells were large and resembled macrophages. Interestingly, viral antigen did not localize in the glandular epithelium, smooth muscle cells, or blood vessels from tissues of the reproductive tract (Fig. 3). Furthermore, EAV antigen was not identified in testes, ductus deferens, pelvic urethra, penis, kidneys, ureters, or urinary bladder (Fig. 2B). The ampullae contained the highest number of EAV antigen-positive cells, and scores ranged from 2 to 4 (≤ 250 positive cells) while other accessory sex glands had scores of 2 or less (≤ 45 positive cells) (Fig. 2B). Median immunostaining scores showed a strong positive correlation with mean viral titers ($\rho = 0.62$).

Tissues derived from most of the stallions that stopped shedding EAV during the course of the study did not exhibit EAV antigen, with the exception of rare EAV antigen-positive stromal cells observed in the left vesicular gland, prostatic lobe, and bulbourethral gland (L137), and left bulbourethral gland (L138 and L142) from three stallions within this group (data not shown). EAV nucleic acids were detected only in the aforementioned tissues from stallion L137 by EAV-specific RT-iiPCR but not in tissues derived from the other two animals. In addition, neither infective virus nor viral nucleic acids were detected in semen samples collected prior to euthanasia, further confirming that there was no active shedding of EAV in these stallions.

Cellular tropism of EAV during persistent infection in the reproductive tract of the stallion. Identification of EAV host cell tropism during persistent infection was assessed in the ampullae, which demonstrated the highest viral infectivity titers and highest number of EAV antigen-positive cells. Both stromal cells and lymphocytes were dually stained for vimentin and EAV N protein (Fig. 4). In contrast, EAV N protein was not detected in the glandular epithelium (vimentin negative and pan-cytokeratin positive) (Fig. 4), which further confirmed the observation that EAV does not persist in the reproductive epithelium. EAV antigen-positive lymphocytes were identified by the expression of the T lymphocyte markers CD2, CD3, CD5 (data not shown), and CD8 (Fig. 4) and by the expression of the B lymphocyte marker CD21 (Fig. 4). Interestingly, viral antigen was not detected in CD4⁺ T lymphocytes (Fig. 4) or tissue macrophages and dendritic cells expressing either CD163 or Iba-1 (ionized calcium-binding adapter molecule 1) (data not shown).

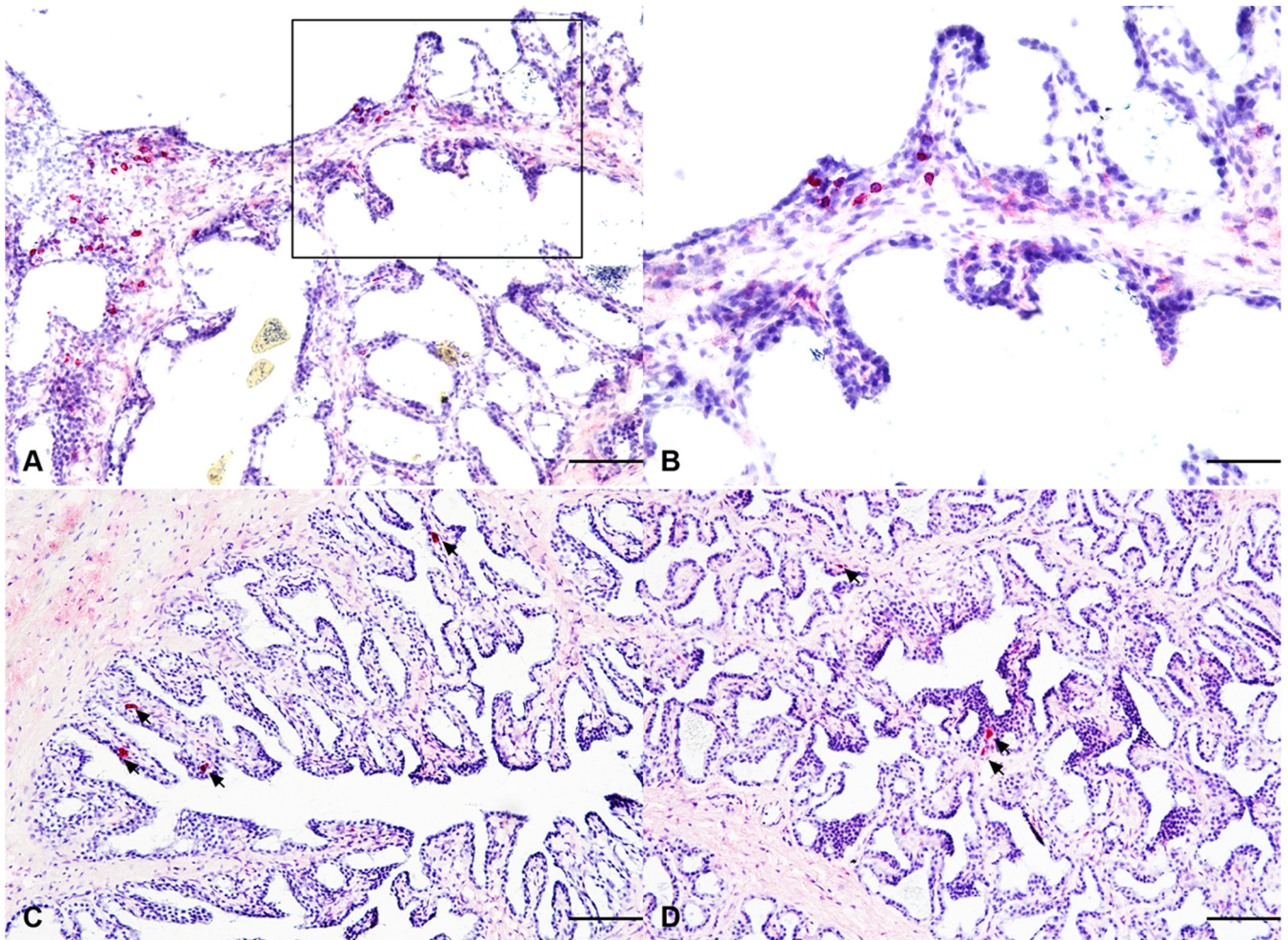


FIG 3 Detection of EAV antigen-positive cells in the accessory sex glands of long-term persistently infected stallions by immunohistochemistry. Tissue sections were stained with an EAV N protein-specific monoclonal antibody (3E2) and a Bond Polymer Refine Red Detection kit. IHC staining was performed with Fast Red. (A) Ampulla. EAV antigen-positive lymphocytes (Fast Red) were either present in inflammatory infiltrates or scattered in the lamina propria. (B) Magnification of the boxed area shown in panel A. EAV antigen-positive lymphocytes (arrowheads) observed in close association with the glandular epithelium. (C) Prostate. Scattered EAV antigen-positive stromal cells (arrowheads) were observed. (D) Bulbourethral gland. Rare stromal cells positive for EAV antigen (arrowheads) were observed. Magnifications, $\times 200$ (A, C, and D) and $\times 400$ (B); bars, $100\ \mu\text{m}$ (A, C, and D) and $50\ \mu\text{m}$ (B).

TEM demonstrates EAV in the ampullae of the stallion. Electron-dense, spherical particles consistent with EAV virion morphology were observed by transmission electron microscopy (TEM) in thin sections from the ampullae of long-term persistently infected stallions and were localized within the cisternae of the endoplasmic reticulum (ER) and other intracellular membrane compartments of fibrocytes. In addition, vesicles containing viral particles were observed in lymphocytes localized within inflammatory infiltrates (Fig. 5). EAV virions had an average size of $59.3\ \text{nm} \pm 8.98\ \text{nm}$. Smaller particles ranging from 42 to 46 nm were also observed and might correspond to immature virions.

Local inflammatory response to persistent EAV infection in the male reproductive tract. There were no significant gross lesions in the reproductive tract of the long-term carrier stallions or in most of the stallions that had stopped shedding EAV in semen. However, gross lesions were observed in the reproductive tract of only one stallion (L139) that had stopped shedding EAV in semen. In this stallion, there were fibrous adhesions between the tunica albuginea of the testis and the tunica vaginalis, a unilateral varicose pampiniform plexus, and a unilateral suppurative epididymitis. Histopathological examination revealed a bilateral, moderate, multifocal lymphoplasmacytic ampullitis with median severity and distribution scores of 3 (301 to 500

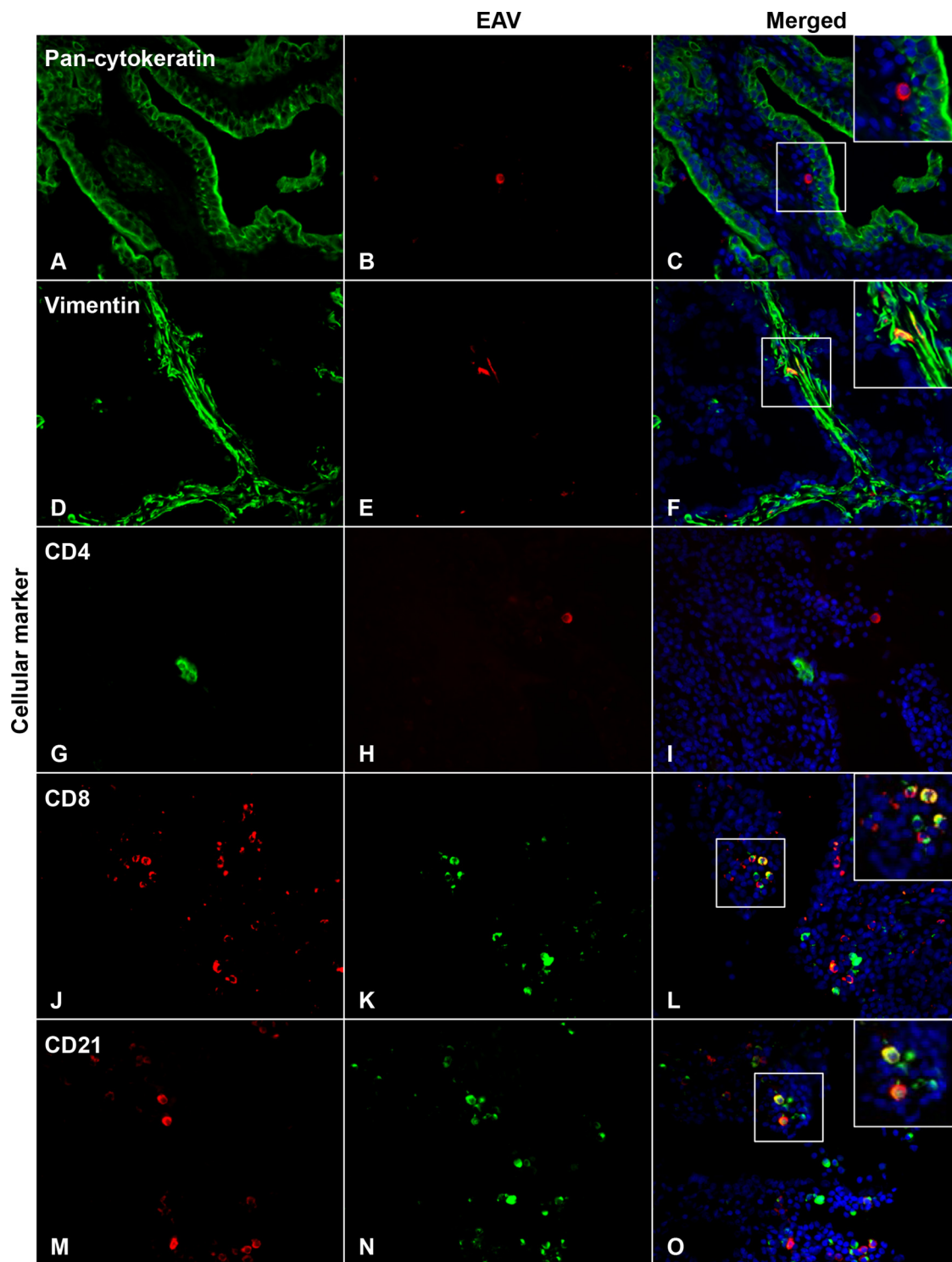


FIG 4 Dual immunofluorescence staining of ampulla sections from long-term persistently infected stallions for EAV antigen and cell surface markers. The cell surface markers (pan-cytokeratin, vimentin, CD4, CD8, and CD21) are identified in panels in the left column of the figure. Staining for the other panels is as indicated above the columns. (A to C) Viral antigen (Alexa Fluor 594, red) is absent in pan-cytokeratin-positive epithelial cells (Alexa Fluor 488, green). (D to F) EAV antigen (Alexa Fluor 594, red) is present in scattered vimentin-positive stromal cells (Alexa Fluor 488, green; merged image shown as yellow). (G to I) EAV antigen (Alexa Fluor 594, red) was not detected in CD4⁺ T lymphocytes (fluorescein isothiocyanate; green). (J to L) EAV antigen (Alexa Fluor 488, green) was detected in a subpopulation of CD8⁺ T lymphocytes (R-phycoerythrin, red; merged image shown as yellow). (M to O) EAV antigen (Alexa Fluor 488, green) was detected in a subpopulation of CD21⁺ B lymphocytes (R-phycoerythrin, red; merged image shown as yellow). Nuclei counterstaining was performed using DAPI (blue). Magnification, $\times 400$.

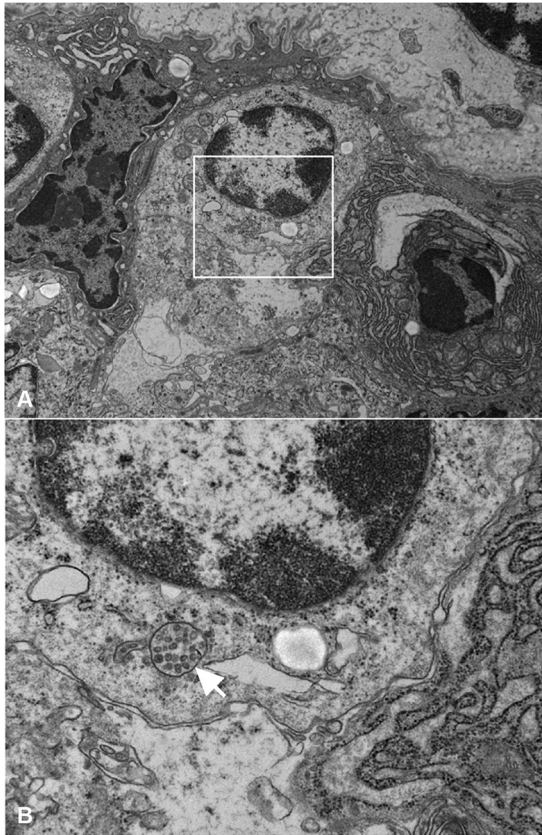


FIG 5 Demonstration of EAV subcellular localization by transmission electron microscopy (TEM). (A) Lymphocyte containing EAV virions within an intracytoplasmic vesicle. The cell was located in an inflammatory infiltrate of the ampulla. Magnification, $\times 9,300$. (B) Magnification ($\times 30,000$) of the boxed area in panel A showing an intracytoplasmic vesicle containing viral particles (arrowhead).

inflammatory cells) and 4 (5 or more foci per tissue section), respectively, in long-term, persistently infected stallions (Fig. 6). Inflammatory mononuclear cells were present as multifocal aggregates within the lamina propria, with a more dispersed distribution pattern between aggregates. The inflammation was particularly prominent within the lamina propria of the luminal villi, and, interestingly, there was a notable presence of intra- and subepithelial CD3⁺ T lymphocytes (Fig. 7). In contrast, the stallions that cleared EAV infection had minimal, focal lymphoplasmacytic ampullitis, with median severity and distribution scores of 1 (31 to 150 inflammatory cells) and 2 (2 foci per tissue section), respectively (Fig. 6). While a moderate number of foamy macrophages were observed infiltrating the ampullae of three stallions that stopped shedding virus (stallions L137, L139, and L141) (Fig. 8), none was observed in tissues derived from persistently infected stallions. Statistical analysis demonstrated significant differences in severity, distribution, and cumulative scores between persistently infected stallions and those that cleared viral infection (Kruskal-Wallis test, P values of ≤ 0.0001) for inflammatory infiltrates in the ampullae, while no significant differences were observed between groups for other genital tract tissues including testes, epididymides, and other accessory sex glands (Fig. 6). Other microscopic findings in both groups included unilateral or bilateral, minimal lymphoplasmacytic orchitis and epididymitis with occasional perivascular cuffs and rare hemosiderophages (Fig. 7) and mild lymphoplasmacytic adenitis of bulbourethral glands with occasional foci of inflammatory cells. Inflammatory lesions were infrequent in vesicular glands and prostate.

Characterization of the local inflammatory response by IHC. The inflammatory response to EAV in the ampullae was further characterized by IHC using lymphocyte,

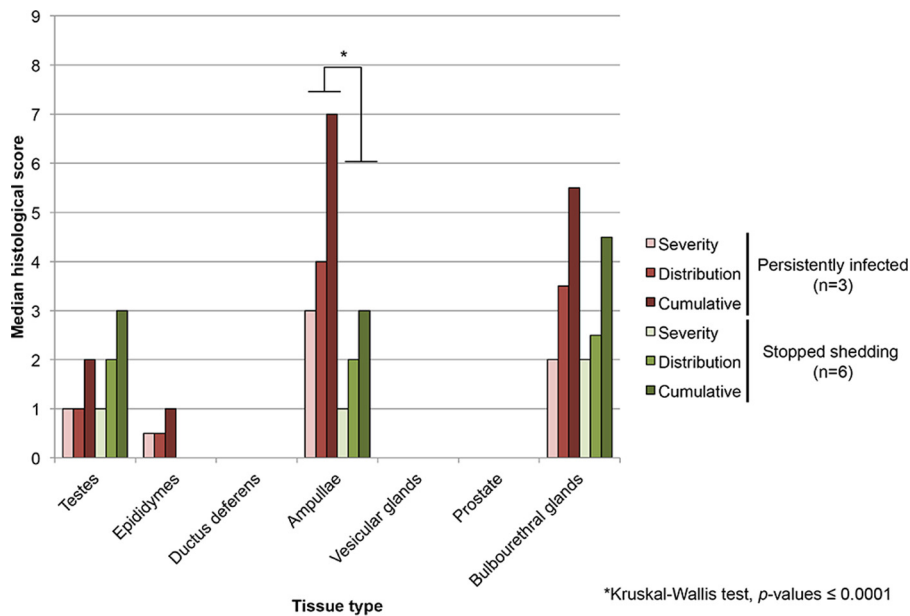


FIG 6 Median histological scores (severity, distribution, and cumulative) per tissue type in EAV long-term persistently infected stallions and stallions that stopped shedding virus in semen during the study ($n = 8$). The severity is categorized as follows: 0, negative (<30 inflammatory cells); 1, minimal (31 to 150 inflammatory cells); 2, mild (151 to 300 inflammatory cells); 3, moderate (301 to 500 inflammatory cells); and 4, severe (>500 inflammatory cells). Distribution scores indicate the following: 0, negative; 1, focal (1 focus per tissue section); 2, rare foci (2 foci per tissue section); 3, occasional foci (3 to 4 foci per tissue section); 4, multifocal (5 or more foci per tissue section); and 5, diffuse. Cumulative scores comprise the sum of both severity and distribution scores, respectively. *, $P \leq 0.0001$, as determined by a Kruskal-Wallis test.

macrophage, and dendritic cell-specific markers (Table 3). The inflammatory response in the ampullae of EAV-infected stallions primarily consisted of T lymphocytes. Statistical analysis demonstrated significant differences in the lymphocyte infiltration between long-term persistently infected stallions and stallions that stopped shedding virus (P values of <0.05). Specifically, infiltrating T lymphocytes in tissues from long-term persistently infected stallions consisted of moderate to high numbers of CD2⁺, CD3⁺, CD5⁺, and CD8⁺ T lymphocytes and low to moderate numbers of CD4⁺ and CD25⁺ T lymphocytes. Clusters of CD21⁺ B lymphocytes were also observed although they comprised a minor component of the inflammatory infiltrates (Table 4 and Fig. 9). In contrast, lymphocytes in tissues from stallions that stopped shedding EAV were comprised of low numbers of CD2⁺, CD3⁺, and CD5⁺ T lymphocytes, rare to minimal CD4⁺ and CD25⁺ T lymphocytes, and low to moderate numbers of CD8⁺ T lymphocytes. CD21⁺ B lymphocytes were either absent or rare in this group (Fig. 9).

A panel of monoclonal and polyclonal antibodies specific for tissue macrophages and dendritic cells was utilized for immunohistochemical characterization of these cells in response to EAV infection (Table 3). This included the following: the leukocyte integrin CD18, reported to be highly expressed in tissue macrophages (44–46); the ionized calcium-binding adapter molecule 1 (Iba-1), a calcium-binding protein expressed in tissue macrophages, dendritic cells, and microglial cells, especially during their activated state (47–49); the major histocompatibility complex class II (MHC-II), an antigen receptor expressed on antigen-presenting cells including tissue macrophages and dendritic cells (50); the scavenger receptors CD163 and CD204, highly expressed in macrophages, especially those with an M2 phenotype (51–54); calprotectin/L1, a marker for activation of macrophages shortly after recruitment from peripheral blood (55, 56); and CD172a, a signal regulatory protein expressed by myeloid-derived cells, including macrophages and other leukocytes (57–62). Monoclonal antibodies directed to the maturation marker CD83 and the costimulatory molecule CD86 were used to

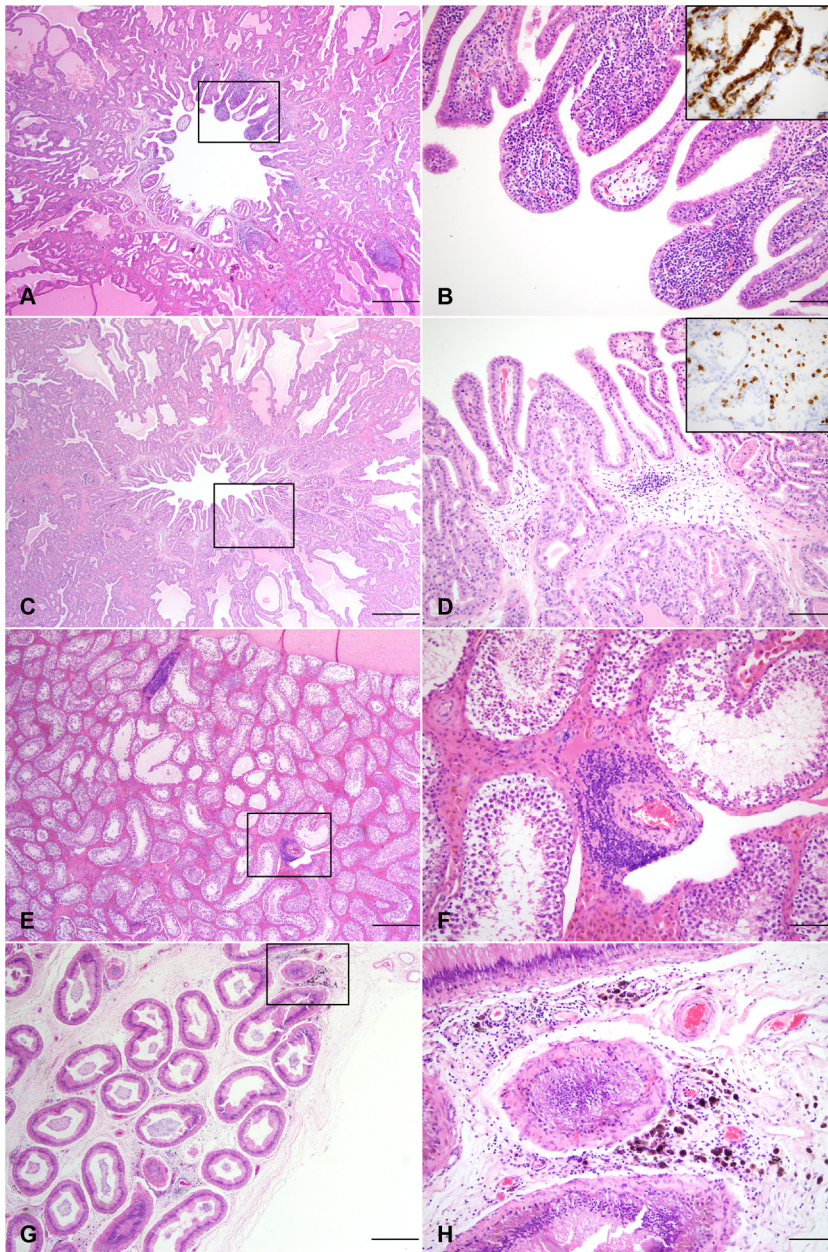


FIG 7 Histological findings following experimental infection of stallions with the EAV KY84 strain. (A) Moderate, multifocal lymphoplasmacytic ampullitis in EAV long-term persistently infected stallions. Magnification, $\times 40$; bar, $500\ \mu\text{m}$. (B) Magnified view of the boxed area in panel A. Note the large predominance of intra- and subepithelial T lymphocytes, as demonstrated by CD3 immunostaining in cryosections from this tissue using a monoclonal antibody to CD3 (LN10) and a Bond Polymer Refine Detection kit (inset, IHC using DAB). Magnification, $\times 200$ (inset, $\times 400$); bar, $100\ \mu\text{m}$ (inset, $50\ \mu\text{m}$). (C) Minimal, focal lymphoplasmacytic ampullitis in stallions that stopped shedding virus during the study. Rare foci of mononuclear cells were present. Magnification, $\times 40$; bar, $500\ \mu\text{m}$. (D) Magnified view of the boxed area in panel C. Note the significantly lower number of CD3⁺ T lymphocytes which are mostly distributed within the lamina propria in contrast to distribution in EAV long-term persistently infected stallions as demonstrated by immunohistochemistry with a monoclonal antibody to CD3 (LN10) and a Bond Polymer Refine Detection kit (inset, IHC with DAB). Magnification, $\times 200$ (inset, $\times 400$); bar, $100\ \mu\text{m}$ (inset, $50\ \mu\text{m}$). (E) Minimal, multifocal, lymphoplasmacytic orchitis with occasional perivascular cuffs in EAV long-term persistently infected stallions. Magnification, $\times 40$; bar, $500\ \mu\text{m}$. (F) Magnified view of the boxed area in panel E depicting a perivascular cuff. Magnification, $\times 200$; bar, $100\ \mu\text{m}$. (G) Mild, multifocal lymphoplasmacytic epididymitis in an EAV long-term persistently infected stallion. Magnification, $\times 40$; bar, $500\ \mu\text{m}$. (H) Magnified view of the boxed area in panel G. Note the presence of hemosiderophages. Magnification, $\times 200$; bar, $100\ \mu\text{m}$. IHC staining was performed with H&E and as noted for panels B and D.

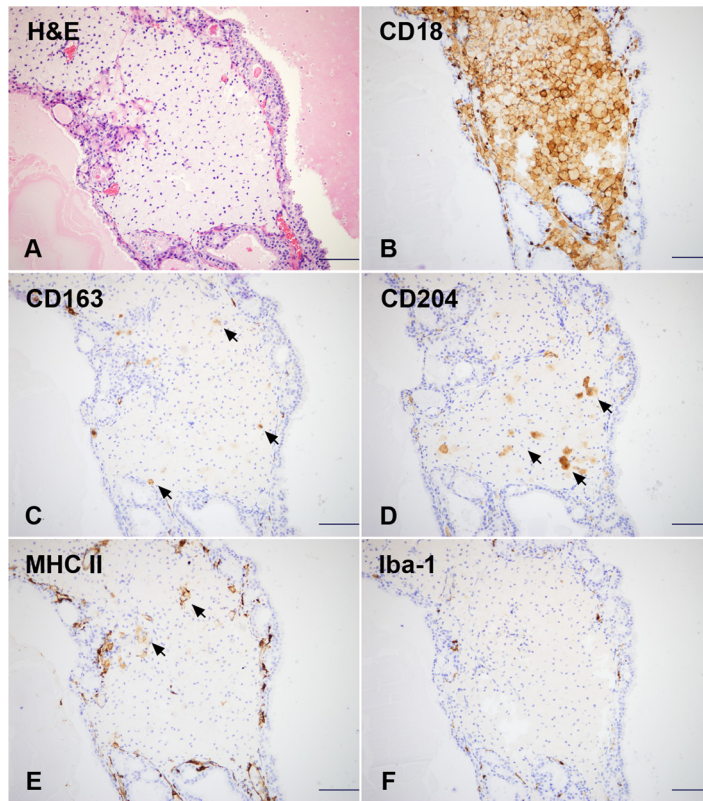


FIG 8 Immunohistochemical characterization of foamy macrophages infiltrating the ampullae from three stallions that stopped viral shedding during the course of the study. Immunohistochemical staining was performed using a panel of monoclonal and polyclonal antibodies specific to macrophage markers and a Bond Polymer Refine Detection kit. (A) Moderate numbers of foamy macrophages infiltrated the lamina propria of the ampullae. Foamy macrophages were CD18⁺ (B), and scattered cells were immunoreactive for CD204 (D, arrowheads). Few foamy macrophages showed immunoreactivity for CD163 (C, arrowheads) and MHC-II (E, arrowheads), whereas none expressed Iba-1 (F). IHC was performed using DAB. Magnification, $\times 200$; bar, 100 μm .

identify dendritic cells (63, 64). Moderate to high numbers of Iba-1⁺ cells along with low to moderate numbers of CD83⁺ cells were observed in tissues derived from long-term, persistently infected stallions (*P* values of <0.05) (Table 5 and Fig. 10). Interestingly, the presence of CD163⁺ and CD204⁺ tissue macrophages in these tissues was low (Fig. 10), while CD86⁺ and calprotectin/L1-positive (calprotectin/L1⁺) cells were rarely identified (Fig. 11). In stark contrast, minimal numbers of Iba-1⁺ or CD83⁺ macrophages and dendritic cells were observed in tissues derived from stallions that stopped shedding virus (Fig. 10). Although CD163 expression was also low in this group, the presence of CD204⁺ tissue macrophages was abundant in some cases (Table 5 and Fig. 10). In common with persistently infected stallions, CD86⁺ and calprotectin/L1⁺ cells were rarely observed in tissues derived from stallions that had stopped shedding virus (Fig. 11). Finally, CD18, CD172a, and MHC-II expression shared similar widespread distributions in tissues derived from both groups (Fig. 11). Immunohistochemical characterization of foamy macrophages observed in tissues derived from three stallions that stopped shedding virus (L137, L139, and L141) revealed that these were CD18⁺, while scattered cells within these infiltrates expressed CD204. In addition, low numbers of foamy macrophages expressed CD163 and MHC-II while none expressed Iba-1 (Fig. 8).

DISCUSSION

Several animal and human viruses have the ability to infect the mammalian male reproductive tract, thereby posing a high risk for sexual transmission (33). In contrast to

TABLE 3 Antibodies for immunohistochemical and immunofluorescent antibody staining used in this study

Cellular phenotype	Antigen	Clone	Assay(s) ^a	Source and reference(s)
T lymphocytes	CD2	HB88A	IHC	Washington State University (W. Davis); 109
	CD3	LN10	IHC	Leica Microsystems; 110
	CD3	UC F6G-3	IFA	University of California (J. L. Stott); 111
	CD4	CV54	IHC and IFA	AbD Serotec; 112
	CD5	HT23A	IHC	Washington State University (W. Davis); 113
	CD8	CV58	IHC and IFA	AbD Serotec; 112
	CD25	4C9	IHC	Leica Microsystems; 110
B lymphocytes	CD21	B-ly4	IHC and IFA	BD Pharmingen; 40
Tissue macrophages and dendritic cells	CD18	CA18.2G1	IHC	University of California (P. F. Moore); 45
	CD83	HB15E	IHC	BD Pharmingen; 114
	CD86	IT2.2	IHC	BioLegend; 114
	CD163	AM-3K	IHC	Transgenic; 115
	CD172a	DH59B	IHC	Washington State University (W. Davis); 16, 71
	CD204	SRA-E5	IHC	Transgenic; 116
	Iba-1	NA ^b	IHC	Wako Chemicals; 48
	MHC-II	CR3/43	IHC	Dako; 117
	Calprotectin/L1	MAC387	IHC	AbD Serotec; 56
Epithelial and mesenchymal cells	Pan-cytokeratin	AE1/AE3	IFA	eBioscience; 118
	Vimentin	V9	IFA	eBioscience; 119

^aIHC, immunohistochemistry; IFA, immunofluorescent antibody staining.

^bNA, not applicable.

many viral infections, EAV has evolved a highly sophisticated mechanism that enables its long-term persistence (carrier state) in the stallion’s reproductive tract with no major associated tissue damage, sperm abnormalities, or adverse effects on reproductive fertility (8, 24, 25). Interestingly, EAV persistence occurs despite induction of host immune responses (e.g., strong neutralizing antibody response) that effectively clear the virus from all body tissues with the exception of the carrier stallion’s reproductive tract (2–4, 8, 18, 24–28, 30). The strategy employed by EAV to successfully evade host

TABLE 4 Immunohistochemical characterization of lymphocyte infiltrates in sections from the ampullae of EAV long-term, persistently infected stallions and stallions that stopped shedding virus in semen

Stallion group and identification	Marker profile by cell type ^a						
	T lymphocytes ^b						B lymphocytes (CD21) ^c
	CD2	CD3	CD4	CD5	CD8	CD25	
Persistently infected							
L136	++++	++++	+++	++++	++++	+++	+++
L140	+++	+++	++	+++	+++	+++	++
Stallion E	+++	++++	++	+++	++++	++	+
Stopped shedding							
L137	++	++	+	++	+++	+/-	-
L138	++	++	+	++	+++	+/-	-
L139	++	++	+	++	++	+	+/-
L141	++	++	+/-	++	++	+	-
L142	++	++	+	++	++	+/-	-
L143	++	++	+	++	+++	+/-	+/-

^aScores reflect the cumulative number of positive cells in five ×100 (total magnification) fields. For all values, *P* < 0.05.

^bFor CD2, CD3, CD4, CD5, and CD8, immunohistochemical scoring is as follows: -, no specific positive cells; +/-, rare presence of positive cells; +, ≤200 positive cells; ++, 201–350 positive cells; +++, 351–500 positive cells; +++++, >500 positive cells. For CD25, immunohistochemical scoring is as follows: -, no specific positive cells; +/-, rare presence of positive cells; +, ≤30 positive cells; ++, 31–80 positive cells; +++, 81–200 positive cells; +++++, >200 positive cells.

^cFor CD21, immunohistochemical scoring is as follows: -, no specific positive cells; +/-, rare presence of positive cells; +, 1 focus of positive cells; ++, 2 foci of positive cells; +++, 3–4 foci of positive cells; +++++, >4 foci of positive cells.

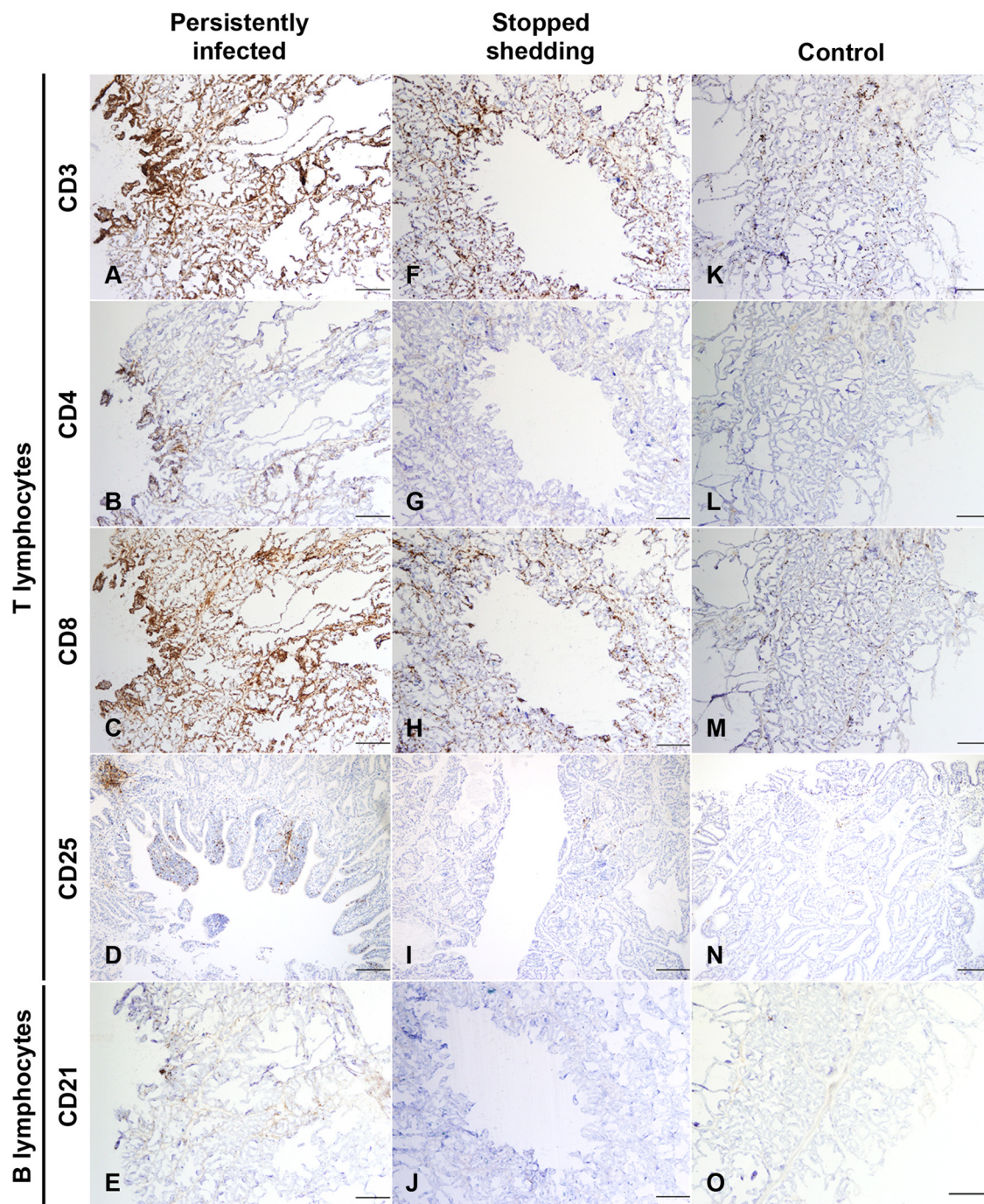


FIG 9 Immunophenotypic characterization of lymphocyte infiltrates in the ampullae of EAV experimentally infected stallions. Immunohistochemical staining was performed using a panel of monoclonal antibodies specific to T and B lymphocyte surface markers and a Bond Polymer Refine Detection kit. Surface markers for T (CD3, CD4, CD8, and CD25) and B (CD21) lymphocytes are indicated to the left. Stallion groups are indicated at the top of the columns. IHC was performed with DAB. Magnification, $\times 40$; bar, 500 μm .

immune surveillance has yet to be determined. Since the carrier stallion plays a pivotal role in the epidemiology of EAV and constitutes the main challenge for its control and potential eradication (2–4, 18, 27), it is important to fully understand the underlying mechanisms involved in the establishment and maintenance of persistent infection in the stallion’s reproductive tract. Until the experiments described herein, our knowledge regarding the anatomical sites of EAV persistence was limited to a single study conducted by infecting pre- and peripubertal colts (≤ 12 months of age) rather than

TABLE 5 Immunohistochemical characterization of tissue macrophages and dendritic cell populations in sections from the ampullae of EAV long-term, persistently infected stallions and stallions that stopped shedding virus in semen

Stallion group and identification	IHC score by marker ^a								
	CD18	CD83 ^b	CD86	CD163	CD172a	CD204	Iba-1 ^b	MHC-II	Calprotectin/L1
Persistently infected									
L136	++++	+++	+	+	++++	++	++++	+++	+/-
L140	+++	++	-	+	+++	++	+++	+/-	+/-
Stallion E	++++	++	-	+	+++	+	+++	++++	+/-
Stopped shedding									
L137	++++	+/-	-	++	+++	++++	+	+++	-
L138	+	+/-	+	+	++	++	+	++	+/-
L139	+++	+/-	+	++	+++	+++	+	+++	+/-
L141	++++	-	-	++	++	+++	+	+/-	+/-
L142	+	+	+/-	+	+	++	+	++	+/-
L143	++	-	-	+	++	++	+	++	+

^aFor CD18, CD163, CD172a, CD204, Iba-1, MHC-II, and calprotectin/L1, immunohistochemical scoring is as follows: -, no specific positive cells; +/-, rare presence of positive cells; +, ≤200 positive cells; ++, 201–350 positive cells; +++, 351–500 positive cells; +++++, >500 positive cells. For CD83 and CD86, immunohistochemical scoring is as follows: -, no specific positive cells; +/-, rare presence of positive cells; +, ≤80 positive cells; ++, 81–120 positive cells; +++, 121–150 positive cells; +++++, >150 positive cells. Scores reflect the cumulative number of positive cells in five ×100 (total magnification) fields.
^bP < 0.05.

sexually mature stallions (43). Moreover, the conclusion that EAV can be isolated only from the ampullae in carrier stallions is based on tissues harvested from a single animal that at 450 dpi was still actively shedding EAV in semen. The remaining animals used in that study were euthanized too early following infection to be reliably classified as persistently infected. Consequently, this earlier study is limited by the fact that it not only employed virus isolation techniques on homogenized tissue samples but also used a very small sample size. Here, we sought to expand our understanding of the pathogenesis of EAV persistence by precisely identifying its anatomic distribution and host cell tropism in the male genital tract following infection of sexually mature stallions. An additional aim was to determine if local host inflammatory responses were associated with chronic EAV infection and to immunophenotype the cells involved.

Direct virus isolation and viral nucleocapsid immunostaining unambiguously demonstrated that EAV anatomic distribution in the reproductive tract of persistently infected stallions is not reliant on immunologically privileged tissues such as the testes but, instead, predominantly involves the accessory sex glands, with the ampullae serving as the major reservoirs for the virus. Within these tissues, EAV exhibited a strong host cell tropism for vimentin-positive stromal cells of the lamina propria (including fibrocytes and possibly tissue macrophages) in addition to T (CD2⁺, CD3⁺, CD5⁺, and CD8⁺) and B (CD21⁺) lymphocytes that were closely associated with local inflammatory infiltrates. Glandular epithelial cells (cytokeratin positive) did not contain detectable amounts of EAV N protein despite the intimate association of EAV-infected intra- and subepithelial lymphocytes with the reproductive epithelium. Even though this close association suggests that infectious virus may gain access to seminal fluid via these infected lymphocytes simply migrating across the glandular epithelium, further investigations are required to test this hypothesis. In addition, EAV was not detectable in lymphoid tissues, including those associated with lymph drainage from the reproductive tract. While this suggests that infected T and B lymphocytes may exhibit a specific homing pattern to the reproductive tract (65–70) and restricted migration from reproductive tract tissues to secondary lymphoid organs, this observation warrants further investigation to better understand the unique mechanism(s) of lymphocyte homing to the male reproductive tract.

Interestingly, results presented here suggest that EAV exhibits different host cell tropism profiles dependent on the tissue compartment and/or stage of infection (i.e., acute versus chronic). For example, while CD21⁺ B lymphocytes containing EAV N antigen are clearly present in the accessory sex glands of the stallion's reproductive tract, recent *in vitro* studies demonstrated that although EAV infects CD3⁺ (CD4⁺ and

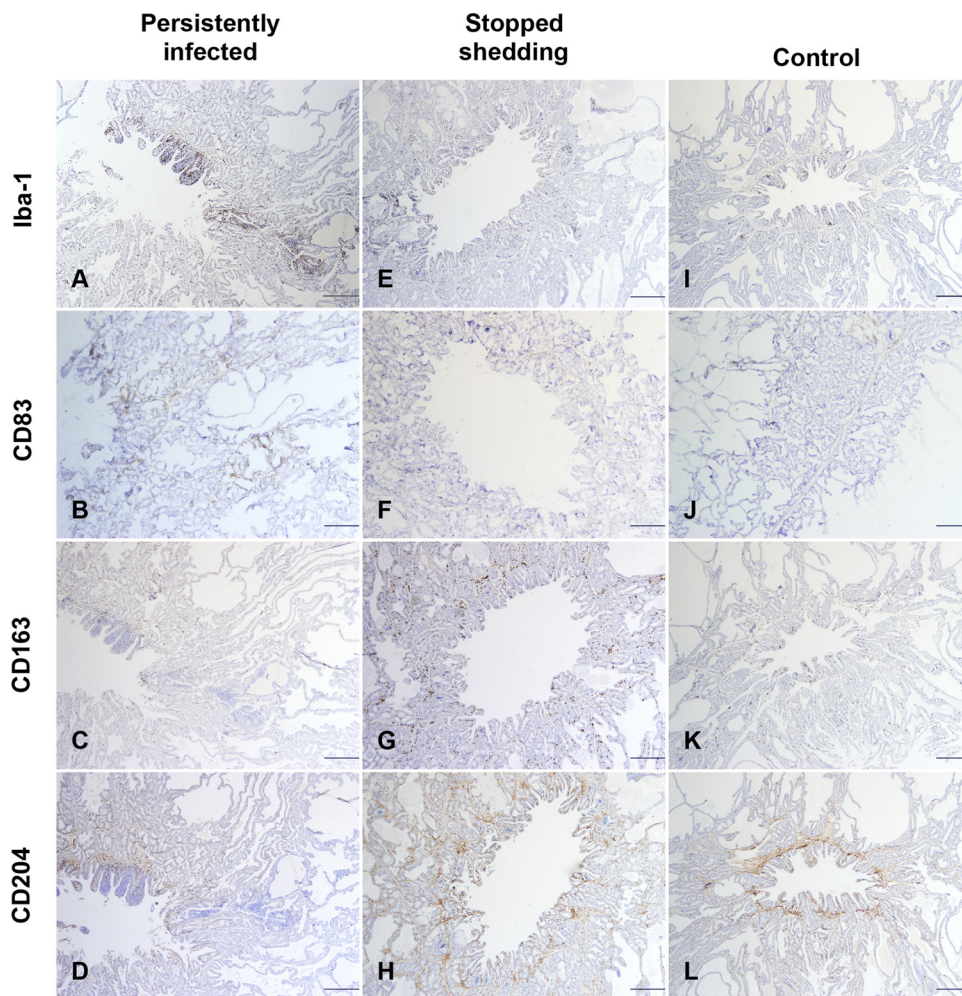


FIG 10 Immunophenotypic characterization of macrophage and dendritic cell infiltrates in the ampullae of EAV experimentally infected stallions. Immunohistochemical staining was performed using a panel of monoclonal and polyclonal antibodies specific to tissue macrophage and dendritic cell markers and a Bond Polymer Refine Detection kit. Specific markers for tissue macrophages and dendritic cells are indicated to the left. Stallion groups are indicated at the top of the columns. IHC was performed with DAB. Magnification, $\times 40$; bar, 500 μm .

CD8⁺) T lymphocytes and CD14⁺ monocytes, it does not infect CD21⁺ B lymphocytes derived from the peripheral blood mononuclear cell fraction (40). However, EAV-infected IgM⁺ B lymphocytes are detectable in both *in vitro* studies conducted using polarized upper respiratory tract mucosal explants and *in vivo* studies during acute infection (16, 71), indicating that infection of these cells is dependent on as yet undiscovered cellular factors. Another significant example of apparent differences in the spectra of EAV host cell tropism is observed during the early and persistent phases of infection. Following initial exposure, EAV N antigen is readily detectable in vascular endothelial cells from small blood vessels, resulting in an extensive panvasculitis, a hallmark of the acute phase of EAV infection (11–13, 15, 72, 73). In contrast, EAV N antigen was not observed in endothelial cells within the reproductive tract of carrier stallions, and no other microscopic lesions except lymphoplasmacytic inflammation are associated with the carrier state. Taken together, our findings suggest variation between peripheral blood and tissue T and B lymphocytes regarding their susceptibility to EAV infection along with clear differences in EAV cell tropism between acute and chronic (persistent) phases of infection. At present, the mechanisms that determine these differences are unknown.

The intimate localization of EAV-infected cells within inflammatory infiltrates indicates that viral replication occurs despite the presence of an inflammatory/immune

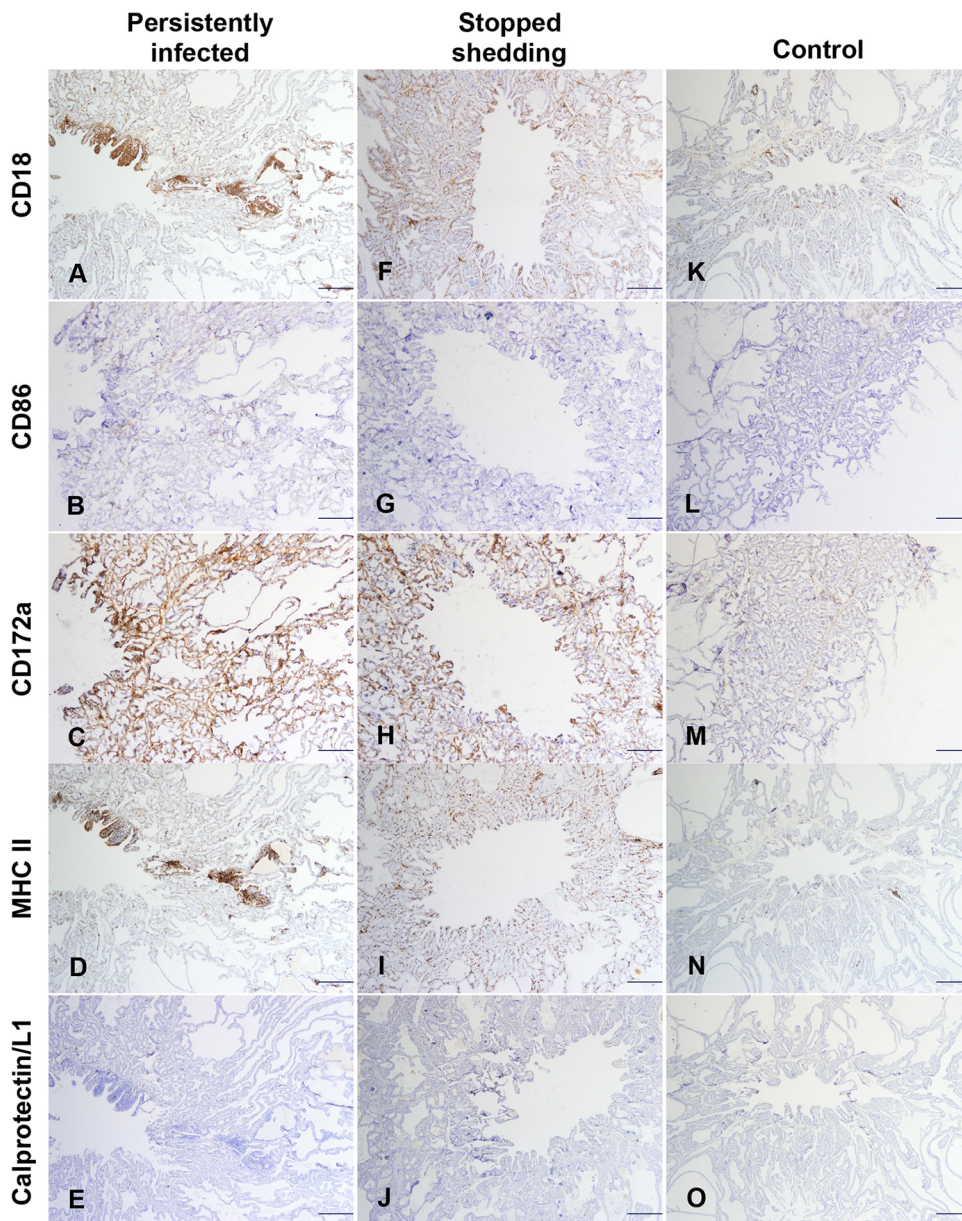


FIG 11 Immunophenotypic characterization of macrophage and dendritic cell infiltrates in the ampullae of EAV experimentally infected stallions (continued). Specific markers for tissue macrophages and dendritic cells are indicated to the left. Stallion groups are indicated at the top of the columns. IHC was performed with DAB. Magnification, $\times 40$; bar, 500 μm .

response in the reproductive tract of persistently infected stallions. This host response was characterized by the presence of mature dendritic cells as defined by expression of CD83, a protein that is essential for T lymphocyte costimulation (63), and by substantial infiltration of CD3⁺ CD5⁺ CD8⁺ T lymphocytes consistent with a cytolytic response. However, only low numbers of these T lymphocytes expressed granzyme B or interferon gamma, suggesting a local suppression in the CD8⁺ T-mediated response (M. Carossino and U. B. R. Balasuriya, unpublished data). Such immunosuppression might be explained by the presence of CD4⁺ CD25⁺ T lymphocytes within the inflammatory infiltrates as this cell phenotype is consistent with T regulatory (Treg) lymphocytes. Support for this notion is provided by the fact Treg cells have been implicated in the suppression of local immune responses following infection with other arteriviruses (74–79). In addition to potential Treg cell activity, EAV undergoes antigenic drift (26, 30)

during the course of persistent infection in carrier stallions that could contribute to immune evasion and/or promote immune exhaustion, as observed for other chronic viral infections (80–84). Another property of the inflammatory response to EAV in the stallion's reproductive tract is that although tissue macrophages were activated as defined by expression of Iba-1 (47, 49), they did not express calprotectin/L1, a marker frequently downregulated in resident macrophages compared with levels in macrophages that have been recently recruited to a tissue site (55). This is consistent with some form of active inhibition of macrophage recruitment to locations in the stallion reproductive tract where EAV replication is occurring. However, further investigations are required to validate this conclusion. Finally, local immune suppression is likely to be enhanced by the strong influence of androgens in reproductive tissue homeostasis (85), which may also explain EAV's dependence on androgenic hormones during persistent infection. Therefore, it is hypothesized that EAV persistence is likely to be associated with dysregulation of local immune responses at multiple levels. Consequently, experiments are in progress to understand the local immune pathways, expand the phenotypic identity of local CD4⁺/CD25⁺ T lymphocytes, and understand the role of androgenic hormones in EAV persistence.

As observed during natural infection, some of the experimentally infected stallions ceased shedding EAV in semen, suggesting that they were capable of clearing the virus from the reproductive tract. Although no infective virus could be isolated from genital tract tissues or semen of these stallions after interruption of viral shedding, very low numbers of stromal cells expressing EAV antigen and containing viral RNA were detectable. This observation is consistent with a previous study from this laboratory (72) and the fact viral RNA can be detected in semen for variable periods of time after the cessation of infectious virus shedding (86, 87). Similar findings have also been reported in the case of other persistent viral infections such as foot-and-mouth disease virus (FMDV) (88–90). However, it was consistently noted that stallions that had stopped shedding had reduced local inflammatory responses compared with those of animals that remained EAV carriers. This reinforces the view that viral replication in the stallion reproductive tract induces a chronic inflammatory state that may aid viral persistence by ensuring the continuous recruitment of lymphocytes as potential susceptible host cells.

Although the mechanisms that determine why some stallions clear the virus from the reproductive tract while others become carriers is far from being fully understood, we have recently demonstrated that the ability of EAV to persist is strongly influenced by host genetics (42). In support of this conclusion it was initially shown that long-term persistence of EAV in the stallion reproductive tract is strongly correlated with possession of a subpopulation of CD3⁺ T lymphocytes that is susceptible to EAV infection *in vitro* (39). Subsequent advanced genetic studies revealed that CD3⁺ T lymphocyte susceptibility or resistance to EAV is controlled by different alleles of the equine homolog encoding the CXCL16 chemokine (SR-PSOX class G [91], located on equine chromosome 11 [ECA11]). These alleles differ by four nonsynonymous nucleotide substitutions within exon 1. The resultant proteins associated with CD3⁺ T lymphocyte EAV susceptibility or resistance are designated CXCL16S and CXCL16R, respectively (41, 42). Furthermore, genetic association studies have demonstrated the correlation between CXCL16S and EAV carrier status in stallions. Moreover, we have determined that CXCL16S has receptor activity for EAV whereas CXCL16R does not (42, 92). Therefore, CXCL16S clearly plays a central role in the establishment and maintenance of persistent infection in the stallion reproductive tract. To fully elucidate this role, analysis of the expression of CXCL16S and its unique receptor (CXCR6) in different cell types within the reproductive tract of carrier stallions is under way in this laboratory. In humans and mice, CXCL16 is expressed in a variety of cell types in different tissues and under different disease conditions (e.g., inflammation or neoplasia) (93–96). CXCL16 is also involved in homing/recruitment of T lymphocytes, plasma cells, and other inflammatory cells (97–99). However, while CXCL16S is clearly an important factor in the establishment and maintenance of persistent

infection, its expression may not be limited solely to the stallion reproductive tract. Therefore, in the context of CXCL16S expression, the stallion reproductive tract must constitute a highly specialized environment with the unique distinction of enabling viral persistence.

In conclusion, the results presented here provide novel insights into the pathogenesis of persistent EAV infection in the reproductive tract of the stallion by identifying tissue reservoirs, viral host cell tropism, and cellular phenotypes involved in local inflammatory responses. They demonstrate that EAV persistence is not dependent on known immunologically privileged sites but appears to involve as yet unidentified mechanisms, potentially including immunosuppression and/or T cell exhaustion to circumvent the antiviral immune responses. Moreover, these results complement our studies on the role of CXCL16S by showing that, in addition to this chemokine, the accessory sex glands must offer a unique microenvironment that supports continuous EAV replication despite elimination of the virus from all other body tissues. The reasons underlying the uniqueness of this microenvironment, along with the immune pathways that lead to viral persistence in the context of CXCL16S expression, are under investigation in our laboratory.

MATERIALS AND METHODS

Cells and viruses. High-passage-number rabbit kidney 13 cells (RK-13 [KY], passage level 399 to 409 [derived from ATCC CCL-37; American Type Culture Collection]) were maintained in Eagle's minimum essential medium (EMEM) (Cellgro; Mediatech, Inc., Herndon, VA) with 10% ferritin-supplemented calf serum (HyClone Laboratories, Inc., Logan, UT), penicillin and streptomycin (100 U/ml and 100 μ g/ml, respectively), and 0.25 μ g/ml of amphotericin B (Gibco, Carlsbad, CA). Equine pulmonary artery endothelial cells (EEC; University of California, Davis, CA) (100) were maintained in Dulbecco's modified essential medium (Mediatech, Herndon, VA) with 1 mM sodium pyruvate, 10% fetal bovine serum (HyClone Laboratories, Inc., Logan, UT), penicillin and streptomycin (100 U/ml and 100 μ g/ml, respectively), 0.25 μ g/ml of amphotericin B, 200 mM L-glutamine, and 0.5 \times nonessential amino acids (Gibco, Carlsbad, CA). Tissue culture fluid (TCF) containing the KY84 strain of EAV (passage 1 in EEC) (University of Kentucky, Lexington, KY) (23) was used for experimental infection of stallions and to infect EEC monolayers for optimization of IHC and IFA assays. The KY84 strain of EAV has been shown to establish persistent infection in the reproductive tract of stallions and to cause moderate clinical signs of EVA in horses (23, 101). The modified live virus (MLV) vaccine strain of EAV (ARVAC; Pfizer Animal Health, Inc., Kalamazoo, MI) was used as the challenge virus in the virus neutralization assay described below.

Ethics statement. This study was performed in strict accordance with the recommendations in the Guide for the Care and Use of Laboratory Animals of the National Institutes of Health. The Institutional Animal Care and Use Committee (IACUC) at the University of Kentucky, Lexington, KY, approved this protocol (number 2011-0888). Stallions were humanely euthanized by pentobarbital overdose according to the American Veterinary Medical Association (AVMA) guidelines for the euthanasia of animals, and all efforts were made to minimize suffering.

Stallions. A total of 13 sexually mature stallions were included in the study (Table 1). These were obtained from UK Maine Chance Farm, University of Kentucky, Lexington, KY. Twelve stallions, including the animals in the control group, were confirmed seronegative (titer of <1:4) before initiation of the study according to the World Organization for Animal Health (Office International des Epizooties [OIE]) standardized protocol (102) described below. An additional stallion naturally infected with EAV during the 2006-2007 multistate EVA outbreak in the United States (31) and classified as a long-term persistently infected stallion was also included in the study. The stallions were housed in individual stalls in an isolation facility for the duration of the study at the University of Kentucky in Lexington, KY.

Experimental infection and establishment of EAV long-term persistent infection (carrier state) in stallions. Eight stallions (animals L136 to L143) were intranasally inoculated in October 2011 with the KY84 strain of EAV (3.75×10^5 PFU per ml of TCF delivered in 5 ml of EMEM) using a fenestrated catheter and monitored as previously described (19, 103). The control group (stallions N105, N121, O103, and O113) remained unexposed and unvaccinated against EAV. Serum neutralizing antibody titers, viremia, and nasal shedding of EAV were assessed by collecting serum, whole blood, and nasopharyngeal swabs at 0, 2, 4, 6, 8, 10, 12, 14, 21, 28, 35, 42, and 726 (pre-euthanasia) days postinfection (dpi) with Vacutainer serum and EDTA tubes (BD, Franklin Lakes, NJ) and sterile rayon swabs (1/2 by 1 in.) with plastic shafts (16 in.), respectively. Nasopharyngeal swabs were placed into virus transport medium (VTM) containing penicillin and streptomycin (100 U/ml and 100 μ g/ml, respectively), 150 mg/liter of gentamicin sulfate (Cellgro; Mediatech, Inc., Herndon, VA), and 0.25 μ g/ml of amphotericin B (Gibco, Carlsbad, CA). Semen samples were collected with the use of an artificial vagina to evaluate viral shedding during the acute phase and after clinical recovery at -2 (prechallenge), 1, 3, 5, 7, 9, 11, 13, 15, 23, 44, and 65 dpi. For the purpose of monitoring viral persistence in the reproductive tract, semen samples were collected approximately once a month, specifically on 86, 107, 128, 149, 170, 198, 226, 254, 282, 317, 345, 380, 407, 448, 462, 476, 497, 548, 701, and 726 dpi. Samples (whole blood, nasopharyngeal swabs, and semen) were processed for virus isolation (VI) as previously described (20). Briefly, nasopharyngeal swabs in VTM were centrifuged at $500 \times g$ for 10 min at 4°C to eliminate cellular debris, filtered through a 0.45- μ m-

TABLE 6 Reproductive, urinary, and lymphoid tissues collected from stallions at postmortem examination

Tissue type	Section(s) ^b
Testis ^a	Cranial, middle, and caudal
Epididymis ^a	Head, body, and tail
Ductus deferens ^a	Proximal, middle, and distal
Ampulla ^a	Proximal, middle, and distal
Vesicular gland ^a	NA
Prostate ^a	NA
Bulbourethral gland ^a	NA
Pelvic urethra	NA
Penis	Pelvic section, shaft, and glans
Kidney ^a	NA
Ureter ^a	NA
Urinary bladder	Fundus and trigonum
Inguinal lymph node ^a	Superficial and deep
Lumbar lymph node ^a	NA
Iliac lymph node ^a	NA
Splenic lymph node	NA
Spleen	NA
Bone marrow	NA

^aLeft and right sides were collected.

^bThe designations proximal and distal are in reference to the relative distances to the inguinal ring, with proximal being closer to it. Other body tissues were collected and examined (not listed), including respiratory tract tissues, visceral organs, lymph nodes, and tonsils. NA, not applicable.

pore-size syringe filter, and stored at -80°C . Whole-blood samples were centrifuged at $500 \times g$ for 10 min, plasma and buffy coat cells were aspirated and placed in a 15-ml conical centrifuge tube, and buffy coat cells were pelleted by centrifugation at $1,500 \times g$ for 10 min at 4°C . The cell pellet was resuspended in 2 ml of EMEM and stored at -80°C .

VNT. Seroconversion was evaluated by a virus neutralization test (VNT) as described in the OIE *Manual for Diagnostics and Vaccines for Terrestrial Animals* (102). A working dilution containing 100 50% tissue culture infective doses (TCID₅₀) per 25 μl of the commercial live-attenuated vaccine strain of EAV (MLV, ARVAC; Zoetis, Kalamazoo, MI) was used as the challenge virus. The use of this strain was based on the existence of a single viral serotype broadly neutralized by polyclonal equine antiserum and on its standardized use for EAV serological testing as indicated in the OIE *Manual of Diagnostic Tests and Vaccines for Terrestrial Animals* (102).

Necropsy examination and tissue collection. Stallions were humanely euthanized by pentobarbital overdose according to the American Veterinary Medical Association (AVMA) guidelines for the euthanasia of animals. Necropsy examination and tissue collection were performed 2 years postinfection. A total of 80 body tissues per stallion, with specific emphasis on the reproductive and urinary tract tissues, regional lymph nodes, and other lymphoid tissues ($n = 50$) (Table 6), were aseptically collected and stored at -80°C . Both right and left sides were sampled in the case of paired organs. In addition, tissues were fixed in 10% neutral buffered formalin for 24 h and paraffin embedded according to standard histological procedures and also snap-frozen in optimum cutting temperature compound (Tissue-Tek O.C.T., Sakura Finetek U.S.A., Torrance, CA). Briefly, individual tissue specimens were placed in a plastic cryo-mold (Tissue-Tek, Sakura Finetek U.S.A., Torrance, CA), covered with O.C.T. compound, and submerged in prechilled 2-methylbutane (Fisher Scientific, Pittsburgh, PA) in liquid nitrogen for 1 min. The frozen tissue block was wrapped in Parafilm (Bemis, Oshkosh, WI) and aluminum foil and then stored at -80°C . Additionally, reproductive tract tissues were fixed in 4% paraformaldehyde and 3.5% glutaraldehyde in 0.1 M Sorensen's buffer for 1.5 h and processed for transmission electron microscopy (TEM) examination.

Virus isolation (VI). Isolation of EAV from raw gel-free semen samples, buffy coat cells, nasopharyngeal swabs, and tissue homogenates was performed according to a standard protocol used by the EAV OIE Reference Laboratory at the Maxwell H. Gluck Equine Research Center, University of Kentucky, as previously described (20, 72, 102, 103). Viral titers were expressed as the number of PFU per milliliter or gram accordingly, and isolates were confirmed by real-time TaqMan reverse transcription-quantitative PCR (RT-qPCR) as previously described (86, 87, 104).

Nucleic acid extraction and reverse transcription-insulated isothermal PCR (RT-iiPCR). Viral nucleic acids were extracted from 10% tissue homogenates and from semen in cases where infective virus could not be isolated but immunopositive cells were detected. A taco mini magnetic bead-based extraction system and RT-iiPCR assay (GeneReach USA, Lexington, MA) were used as previously described (87).

Histopathology. Sections of formalin-fixed paraffin-embedded (FFPE) tissues (5 μm) were stained with hematoxylin and eosin (H&E) according to a standard laboratory procedure prior to histological evaluation. Tissue sections were scrutinized by experienced veterinary pathologists who were blinded as to the carrier status of the stallions, and a morphological diagnosis was provided. Inflammatory lesions received a cumulative score based on their severity and distribution (cumulative score = inflammation severity + inflammation distribution). The severity was categorized according to the cumulative number

of inflammatory cells quantified in five fields at a magnification of $\times 400$ (total magnification) as follows: 0, negative (<30 inflammatory cells); 1, minimal (31 to 150 inflammatory cells); 2, mild (151 to 300 inflammatory cells); 3, moderate (301 to 500 inflammatory cells); and 4, severe (>500 inflammatory cells). Similarly, the distribution was scored as follows: 0, negative; 1, focal (1 focus per tissue section); 2, rare foci (2 foci per tissue section); 3, occasional foci (3 to 4 foci per tissue section); (4), multifocal (5 or more foci per tissue section); and 5, diffuse.

Antibodies. A monoclonal antibody (MAb) specific to EAV N protein (MAb 3E2) was used for IHC and IFA staining as previously described (15, 72). Additionally, a MAb specific to bluetongue virus (BTV) VP7 protein (MAb 290) (105) was used as a negative control. Mouse MAbs and rabbit polyclonal antibodies against several cellular markers were utilized for single and dual IHC and IFA (Table 3). IHC staining was performed using Bond Polymer Refine Detection and Bond Polymer Refine Red Detection kits (Leica Biosystems, Buffalo Grove, IL) as described below. An Alexa Fluor 488- or Alexa Fluor 594-conjugated F(ab')₂ fragment of goat anti-mouse IgG (Life Technologies, Grand Island, NY) was used as the secondary antibody for IFA staining.

EAV anti-nucleocapsid-specific IHC. Snap-frozen tissue sections (10 μm) were mounted on positively charged Superfrost Plus slides (Fisher Scientific, Pittsburgh, PA). Slides were fixed in cold acetone for 10 min and processed with a Leica Bond-Max automated staining system (Leica Biosystems, Buffalo Grove, IL). Immunostaining was performed using MAb 3E2 (1:50 dilution in ISH/IHC Super Blocking [Leica Biosystems, Buffalo Grove, IL]) and a Bond Polymer Refine Red Detection kit (Leica Biosystems, Buffalo Grove, IL) as previously described but omitting the antigen retrieval step (72). Sections were mounted with permanent mounting medium (Micromount; Leica Biosystems, Buffalo Grove, IL). EAV KY84-infected and mock-infected EEC monolayers were used as positive and negative assay controls along with the ampulla of a control stallion. Tissue sections that were not incubated with the primary antibody along with tissue sections stained with BTV VP7-specific MAb were included to assess staining specificity. The cumulative number of positively stained cells was quantified in five $\times 100$ (total magnification) fields using ImageJ, version 1.48, digital image analysis software (National Institutes of Health [NIH], Bethesda, MD) (106) and an ImageJ plug-in for color deconvolution (107). Following deconvolution, a scale was set according to the micrometer scale bar on each image, the images were thresholded, and positive cells were counted. A score was assigned according to the number of immunopositive cells identified as follows: 0, negative; 1, <5 positive cells; 2, 5 to ≤ 45 positive cells; 3, 46 to ≤ 125 positive cells; 4, 126 to ≤ 250 positive cells; and 5, >250 positive cells.

Single IHC for various subpopulations of lymphocytes and tissue specific macrophages. Acetone-fixed frozen sections (10 μm) were prepared as previously indicated. Immunostaining was performed using a Bond Polymer Refine Detection kit (Leica Biosystems, Buffalo Grove, IL). Briefly, endogenous peroxidase activity was blocked after incubation with 0.03% hydrogen peroxide for 15 min, and then sections were washed with $1\times$ phosphate-buffered saline (PBS), pH 7.4 (Gibco, Carlsbad, CA), and incubated with specific MAbs against CD2, CD3, CD4, CD5, CD8, CD21, CD83, CD86, and CD172a (Table 3) for 1 h at room temperature. This was followed by incubation with a rabbit anti-mouse IgG (8 min) and a polymer-labeled goat anti-rabbit IgG conjugated to horseradish peroxidase (HRP) (8 min). DAB (3,3'-diaminobenzidine tetrahydrochloride) was used as the substrate and incubated for 10 min. Finally, sections were counterstained and mounted as previously described.

Sections of FFPE tissues (5 μm) were mounted on positively charged Superfrost Plus slides (Fisher Scientific, Pittsburgh, PA) and dried overnight at 37°C. For retrieval of CD25, CD204, and Iba-1 antigens, heat-induced epitope retrieval (HIER) was performed following automated deparaffinization using a ready-to-use citrate-based solution (pH 6.0; Leica Microsystems, Buffalo Grove, IL) at 100°C for 20 min. For CD18, CD163, MHC-II, and calprotectin/L1 immunostaining, deparaffinization was performed by baking samples in a 60°C oven (ProBlot; Labnet International, Inc., Edison, NJ) for 15 min, followed by two xylene changes (5 min each), incubation in successive ethyl alcohols (100%, 90%, and 80%), and rehydration in $1\times$ PBS. HIER was performed on either a modified citrate-based ready-to-use solution (pH 6.1; Dako, Carpinteria, CA) at 96°C for 30 min (CD18, CD163, and MHC-II antigens) or a $10\times$ citrate-based solution (pH 6.0; Dako, Carpinteria, CA) diluted to $1\times$ in deionized water at 96°C for 30 min (calprotectin/L1 antigen). Slides were allowed to cool for 20 min and washed three times in $1\times$ PBS. Immunostaining was performed using a Bond Polymer Refine Detection kit (Leica Biosystems, Buffalo Grove, IL). The slides were incubated with 3% hydrogen peroxide (5 min), followed by incubation with MAbs specific for CD18, CD25, CD163, CD204, Iba-1, MHC-II, and calprotectin/L1 for 1 h at room temperature. After incubation with the MAbs, the immunostaining procedure was continued as described above for other cellular markers, with the exception of anti-Iba-1, for which the rabbit anti-mouse IgG incubation step was omitted. Positive tissue controls for each cellular marker were included (tonsil, liver, and spleen from control stallions). The cumulative number of immunohistochemical positive cells was quantified in five $\times 100$ (total magnification) fields, and a score was assigned as indicated in Table 7. Expected normal scores for each marker were determined by the number of specifically immunostained cells observed in the tissues from the control group, and IHC scores were normalized accordingly as described under "Statistical analysis" (108).

Dual IHC. Acetone-fixed frozen tissue sections (10 μm) were prepared as previously indicated. Immunostaining was sequentially performed using Bond Polymer Refine Red Detection and Bond Polymer Refine Detection kits. Briefly, the endogenous peroxidase activity was blocked after incubation with 0.03% hydrogen peroxide for 15 min, and tissue sections were incubated with MAb 3E2, followed by the use of a Bond Polymer Refine Red Detection kit as previously described. This was followed by sequential immunostaining using a set of primary antibodies against cellular markers (CD2, CD3, CD5, CD8, CD21, Iba-1, and CD163) and a Bond Polymer Refine Detection kit as indicated above. Finally,

TABLE 7 Scoring system used for specific cellular immunostaining

Score	Interpretation for the indicated marker(s) ^a			
	CD2, CD3, CD4, CD5, CD8, CD18, CD163, CD172a, CD204, Iba-1, MHC-II, and calprotectin/L1 (no. of cells)	CD21 (no. of foci)	CD25 (no. of cells)	CD83 and CD86 (no. of cells)
–	None	None	None	None
+/-	Rare	Rare	Rare	Rare
+	≤200	1	≤30	≤80
++	201–350	2	31–80	81–120
+++	351–500	3–4	81–200	121–150
++++	>500	>4	>200	>150

^aNumerical values express the cumulative number of immunohistochemically positive cells, except as noted, in five ×100 microscopic fields.

sections were counterstained and mounted as indicated previously. Appropriate controls were included as indicated above, in addition to incubation with an isotype control in replacement of the second set of primary antibodies (Sigma-Aldrich, St. Louis, MO) in order to assess staining specificity.

Indirect immunofluorescent antibody (IFA) staining. Snap-frozen tissue sections (10 μm) were obtained as previously indicated. Tissue sections were fixed in 4% paraformaldehyde in 1× PBS for 20 min at room temperature, washed in 1× PBS (three times, 5 min each), permeabilized with 0.1% Triton X-100 (Sigma-Aldrich, St. Louis, MO) in 1× PBS for 15 min at room temperature, and washed as described above. Tissue sections were blocked with ISH/IHC Super Blocking (Leica Biosystems, Buffalo Grove, IL) for 1 h at room temperature in a humidity tray and incubated with MAb 3E2 (diluted 1:50) overnight at 4°C in a humidity tray. Slides were subsequently washed with 1× PBS (four times, 5 min each) and incubated with the secondary antibody [F(ab')₂ fragment of goat anti-mouse IgG conjugated with Alexa Fluor 594 (Life Technologies, Grand Island, NY)] diluted 1:200 in 5% normal goat serum (Jackson ImmunoResearch, West Grove, PA) for 1 h at room temperature in a humidity tray. Finally, sections were washed as described above, and nuclear counterstaining was performed with a mounting medium containing 4',6-diamidino-2-phenylindole (DAPI; Vector Laboratories, Burlingame, CA). Tissue sections were observed under a Nikon Ti fluorescence microscope, and images were acquired using NIS Ar imaging software (Nikon Corporate, Tokyo, Japan). Appropriate controls were used as described for IHC.

Dual IFA staining. Paraformaldehyde-fixed and permeabilized frozen tissue sections (10 μm) were prepared as described above. A sequential immunostaining protocol was developed, which consisted of EAV anti-N staining followed by specific cellular surface marker staining. After the blocking step previously described, the MAb 3E2 was incubated overnight at 4°C in a humidity tray. Slides were subsequently washed with 1× PBS (four times, 5 min each), incubated with the secondary antibody [F(ab')₂ fragment of goat anti-mouse IgG conjugated with Alexa Fluor 488 or Alexa Fluor 594] diluted 1:200 in 5% normal goat serum (Jackson ImmunoResearch, West Grove, PA) for 1 h at room temperature in a humidity tray. The use of Alexa Fluor 488- or Alexa Fluor 594-conjugated secondary antibody (Life Technologies, Grand Island, NY) depended on the fluorochrome conjugated to antibodies specific to cellular markers. Sections were washed as described above, and free binding sites from the goat anti-mouse IgG were blocked with 5% normal mouse serum (Jackson ImmunoResearch, West Grove, PA) for 30 min at room temperature before incubation with the second set of MAbs. Staining of specific cellular surface markers using fluorescence-conjugated MAbs (CD3, CD4, CD8, CD21, pan-cytokeratin, and vimentin) was performed for 1 h at room temperature in a humidity tray. Slides were finally washed, and nuclear counterstaining was performed as previously described. Tissue sections were visualized, and images were captured as described previously; images from different fluorescent channels were overlaid using ImageJ, version 1.48, digital image analysis software (National Institutes of Health [NIH], Bethesda, MD). Appropriate controls were used as described for IHC.

TEM. Samples were fixed as indicated previously, postfixed in 1% osmium tetroxide (OsO₄) for 1.5 h at 4°C, embedded in Eponate 12 (Ted Pella, Inc., Redding, CA), and polymerized for 48 h at 60°C. Ultrathin sections were obtained using a Reichert Ultracut E ultramicrotome (Leica Biosystems, Buffalo Grove, IL), collected on copper grids, and counterstained with 4% uranyl acetate solution and Reynold's lead citrate. Images were obtained using a Philips Tecnai BioTwin 12 transmission electron microscope (TEM) (FEI, Hillsboro, OR).

Statistical analysis. Data distribution, box plots, and scatterplots were generated using JMP10 statistical analysis software (SAS, Cary, NC). All correlation and statistical tests were performed using JMP10 statistical analysis software. Correlation analysis was performed by the Spearman's rank correlation method. Histopathology scores were subjected to statistical analysis of nonparametric data by a Kruskal-Wallis test. In addition, cellular marker immunostaining scores were normalized as performed by Gown et al. (108). The normalized score was generated by subtracting the immunostaining score of tissues derived from control stallions from that of tissues obtained from persistently infected stallions and stallions that stopped shedding virus. The IHC scores for each specific cellular marker were subjected to statistical analysis of nonparametric data by a Kruskal-Wallis test as previously indicated. The level of significance was set at a *P* value of <0.05 in all cases.

ACKNOWLEDGMENTS

This work was supported by Agriculture and Food Research Initiative competitive grant number 2013-68004-20360 from the USDA National Institute of Food and Agriculture (USDA-NIFA) and the Hildegard Rosa Shapiro Endowed Equine Research Fund at the Maxwell H. Gluck Equine Research Center, Department of Veterinary Science, University of Kentucky.

We declare that we have no conflicts of interest.

We gratefully acknowledge Scot Marsh of Leica Microsystems, James Begley, Bruce Maley, Cindy Meier, and Cynthia Long of the UK Imaging Facility, Kirsten Scoggin of the Maxwell H. Gluck Equine Research Center for technical support, Peter F. Moore (Department of Pathology, Microbiology and Immunology, School of Veterinary Medicine, University of California, Davis, CA) for advice on macrophage markers and kindly providing the anti-CD18 monoclonal antibody used in this study, William C. Davis (Monoclonal Antibody Center, College of Veterinary Medicine, Washington State University, Pullman, WA) for kindly providing anti-CD2, -CD5, and -CD172a monoclonal antibodies, Lynn Ennis, Kevin Gallagher, and Felicia Kost of the Gluck Equine Research Center Animal Resources, Diane Furry for assistance in figure preparation, and Kathleen M. Shuck for proofreading the manuscript. We also thank Lakshman Chelvarajan, Sanjay Sarkar, Ashish Tiwari, Yanqiu Li, Pamela Henney, Ashley Skillman, and Casey Edwards for the assistance provided during sample collection.

REFERENCES

- Cavanagh D. 1997. *Nidovirales*: a new order comprising *Coronaviridae* and *Arteriviridae*. *Arch Virol* 142:629–633.
- Balasuriya U, MacLachlan NJ. 2013. Equine viral arteritis, p 169–181. In Sellon DC, Long MT (ed), *Equine infectious diseases*, 2nd ed. Saunders, St. Louis, MO.
- Balasuriya UB, Go YY, MacLachlan NJ. 2013. Equine arteritis virus. *Vet Microbiol* 167:93–122. <https://doi.org/10.1016/j.vetmic.2013.06.015>.
- Balasuriya UBR, Carossino M, Timoney PJ. 10 November 2016. Equine viral arteritis: a respiratory and reproductive disease of significant economic importance to the equine industry. *Equine Vet Educ* <https://doi.org/10.1111/eve.12672>.
- Timoney PJ. 2000. The increasing significance of international trade in equids and its influence on the spread of infectious diseases. *Ann N Y Acad Sci* 916:55–60.
- Timoney PJ. 2000. Factors influencing the international spread of equine diseases. *Vet Clin North Am Equine Pract* 16:537–551.
- Timoney PJ, McCollum WH. 1988. Equine viral arteritis: epidemiology and control. *J Equine Vet Sci* 8:54–59. [https://doi.org/10.1016/S0737-0806\(88\)80112-6](https://doi.org/10.1016/S0737-0806(88)80112-6).
- Timoney PJ, McCollum WH. 1993. Equine viral arteritis. *Vet Clin North Am Equine Pract* 9:295–309.
- Snijder EJ, Meulenbergh JJ. 1998. The molecular biology of arteriviruses. *J Gen Virol* 79:961–979. <https://doi.org/10.1099/0022-1317-79-5-961>.
- Snijder EJ, Kikkert M, Fang Y. 2013. Arterivirus molecular biology and pathogenesis. *J Gen Virol* 94:2141–2163. <https://doi.org/10.1099/vir.0.056341-0>.
- Lopez JW, del Piero F, Glaser A, Finazzi M. 1996. Immunoperoxidase histochemistry as a diagnostic tool for detection of equine arteritis virus antigen in formalin fixed tissues. *Equine Vet J* 28:77–79. <https://doi.org/10.1111/j.2042-3306.1996.tb01593.x>.
- Del Piero F. 2000. Equine viral arteritis. *Vet Pathol* 37:287–296. <https://doi.org/10.1354/vp.37-4-287>.
- Del Piero F. 2000. Diagnosis of equine arteritis virus infection in two horses by using monoclonal antibody immunoperoxidase histochemistry on skin biopsies. *Vet Pathol* 37:486–487. <https://doi.org/10.1354/vp.37-5-486>.
- Bryans JT, Doll ER, Jones TC. 1957. The lesions of equine viral arteritis. *Cornell Vet* 47:52–68.
- MacLachlan NJ, Balasuriya UB, Rossitto PV, Hullinger PA, Patton JF, Wilson WD. 1996. Fatal experimental equine arteritis virus infection of a pregnant mare: immunohistochemical staining of viral antigens. *J Vet Diagn Invest* 8:367–374. <https://doi.org/10.1177/104063879600800316>.
- Vairo S, Favoreel H, Scagliarini A, Nauwynck H. 2013. Identification of target cells of a European equine arteritis virus strain in experimentally infected ponies. *Vet Microbiol* 167:235–241. <https://doi.org/10.1016/j.vetmic.2013.07.020>.
- Vairo S, Vandekerckhove A, Steukers L, Glorieux S, Van den Broeck W, Nauwynck H. 2012. Clinical and virological outcome of an infection with the Belgian equine arteritis virus strain 08P178. *Vet Microbiol* 157:333–344. <https://doi.org/10.1016/j.vetmic.2012.01.014>.
- Balasuriya U. 2014. Equine viral arteritis. *Vet Clin North Am Equine Pract* 30:543–560. <https://doi.org/10.1016/j.cveq.2014.08.011>.
- Balasuriya UB, Snijder EJ, Heidner HW, Zhang J, Zevenhoven-Dobbe JC, Boone JD, McCollum WH, Timoney PJ, MacLachlan NJ. 2007. Development and characterization of an infectious cDNA clone of the virulent Bucyrus strain of equine arteritis virus. *J Gen Virol* 88:918–924. <https://doi.org/10.1099/vir.0.82415-0>.
- Balasuriya UB, Snijder EJ, van Dinten LC, Heidner HW, Wilson WD, Hedges JF, Hullinger PJ, MacLachlan NJ. 1999. Equine arteritis virus derived from an infectious cDNA clone is attenuated and genetically stable in infected stallions. *Virology* 260:201–208. <https://doi.org/10.1006/viro.1999.9817>.
- Campos JR. 2012. Effects on semen quality and on establishment of persistent equine arteritis virus (EAV) infection in stallions following experimental challenge with the Kentucky 84 (KY84) strain. MS thesis. University of Kentucky, Lexington, KY.
- Go YY, Cook RF, Fulgencio JQ, Campos JR, Henney P, Timoney PJ, Horohov DW, Balasuriya UB. 2012. Assessment of correlation between in vitro CD3⁺ T cell susceptibility to EAV infection and clinical outcome following experimental infection. *Vet Microbiol* 157:220–225. <https://doi.org/10.1016/j.vetmic.2011.11.031>.
- McCollum WH, Timoney PJ, Tengelsen LA. 1995. Clinical, virological and serological responses of donkeys to intranasal inoculation with the KY-84 strain of equine arteritis virus. *J Comp Pathol* 112:207–211. [https://doi.org/10.1016/S0021-9975\(05\)80062-3](https://doi.org/10.1016/S0021-9975(05)80062-3).
- Timoney PJ, McCollum WH, Roberts AW, Murphy TW. 1986. Demonstration of the carrier state in naturally acquired equine arteritis virus infection in the stallion. *Res Vet Sci* 41:279–280.
- Timoney PJ, McCollum WH, Murphy TW, Roberts AW, Willard JG, Carswell GD. 1987. The carrier state in equine arteritis virus infection in the stallion with specific emphasis on the venereal mode of virus transmission. *J Reprod Fertil Suppl* 35:95–102.
- Balasuriya UB, Hedges JF, Smalley VL, Navarrette A, McCollum WH, Timoney PJ, Snijder EJ, MacLachlan NJ. 2004. Genetic characterization of equine arteritis virus during persistent infection of stallions. *J Gen Virol* 85:379–390. <https://doi.org/10.1099/vir.0.19545-0>.

27. Balasuriya UBR, Sarkar S, Carossino M, Go YY, Chelvarajan L, Cook RF, Loynachan AT, Timoney PJ, Bailey E. 2016. Host factors that contribute to equine arteritis virus persistence in the stallion: an update. *J Equine Vet Sci* 43 (Suppl):S11–S17.
28. Timoney PJ, McCollum WH. 2000. Equine viral arteritis: further characterization of the carrier state in stallions. *J Reprod Fertil Suppl* 56:3–11.
29. Miszczak F, Legrand L, Balasuriya UB, Ferry-Abitbol B, Zhang J, Hans A, Fortier G, Pronost S, Vabret A. 2012. Emergence of novel equine arteritis virus (EAV) variants during persistent infection in the stallion: origin of the 2007 French EAV outbreak was linked to an EAV strain present in the semen of a persistently infected carrier stallion. *Virology* 423: 165–174. <https://doi.org/10.1016/j.virol.2011.11.028>.
30. Hedges JF, Balasuriya UB, Timoney PJ, McCollum WH, MacLachlan NJ. 1999. Genetic divergence with emergence of novel phenotypic variants of equine arteritis virus during persistent infection of stallions. *J Virol* 73:3672–3681.
31. Zhang J, Timoney PJ, Shuck KM, Seoul G, Go YY, Lu Z, Powell DG, Meade BJ, Balasuriya UB. 2010. Molecular epidemiology and genetic characterization of equine arteritis virus isolates associated with the 2006–2007 multi-state disease occurrence in the USA. *J Gen Virol* 91:2286–2301. <https://doi.org/10.1099/vir.0.019737-0>.
32. McCollum WH, Little TV, Timoney PJ, Swerczek TW. 1994. Resistance of castrated male horses to attempted establishment of the carrier state with equine arteritis virus. *J Comp Pathol* 111:383–388. [https://doi.org/10.1016/S0021-9975\(05\)80096-9](https://doi.org/10.1016/S0021-9975(05)80096-9).
33. Dejuq N, Jegou B. 2001. Viruses in the mammalian male genital tract and their effects on the reproductive system. *Microbiol Mol Biol Rev* 65:208–231. <https://doi.org/10.1128/MMBR.65.2.208-231.2001>.
34. McCarthy M. 2016. Zika virus was transmitted by sexual contact in Texas, health officials report. *BMJ* 352:i720. <https://doi.org/10.1136/bmj.i720>.
35. McCarthy M. 2016. US health officials investigate sexually transmitted Zika virus infections. *BMJ* 352:i1180. <https://doi.org/10.1136/bmj.i1180>.
36. Hills SL, Russell K, Hennessey M, Williams C, Oster AM, Fischer M, Mead P. 2016. Transmission of Zika virus through sexual contact with travelers to areas of ongoing transmission—continental United States, 2016. *MMWR Morb Mortal Wkly Rep* 65:215–216. <https://doi.org/10.15585/mmwr.mm6508e2>.
37. Musso D, Roche C, Robin E, Nhan T, Teissier A, Cao-Lormeau VM. 2015. Potential sexual transmission of Zika virus. *Emerg Infect Dis* 21: 359–361. <https://doi.org/10.3201/eid2102.141363>.
38. Barzon L, Pacenti M, Franchin E, Lavezzo E, Trevisan M, Sgarabotto D, Palu G. 2016. Infection dynamics in a traveller with persistent shedding of Zika virus RNA in semen for six months after returning from Haiti to Italy, January 2016. *Euro Surveill* 21:30316. <https://doi.org/10.2807/1560-7917.ES.2016.21.32.30316>.
39. Go YY, Bailey E, Timoney PJ, Shuck KM, Balasuriya UB. 2012. Evidence that in vitro susceptibility of CD3⁺ T lymphocytes to equine arteritis virus infection reflects genetic predisposition of naturally infected stallions to become carriers of the virus. *J Virol* 86:12407–12410. <https://doi.org/10.1128/JVI.01698-12>.
40. Go YY, Zhang J, Timoney PJ, Cook RF, Horohov DW, Balasuriya UB. 2010. Complex interactions between the major and minor envelope proteins of equine arteritis virus determine its tropism for equine CD3⁺ T lymphocytes and CD14⁺ monocytes. *J Virol* 84:4898–4911. <https://doi.org/10.1128/JVI.02743-09>.
41. Go YY, Bailey E, Cook DG, Coleman SJ, Macleod JN, Chen KC, Timoney PJ, Balasuriya UB. 2011. Genome-wide association study among four horse breeds identifies a common haplotype associated with in vitro CD3⁺ T cell susceptibility/resistance to equine arteritis virus infection. *J Virol* 85:13174–13184. <https://doi.org/10.1128/JVI.06068-11>.
42. Sarkar S, Bailey E, Go YY, Cook RF, Kalbfleisch T, Eberth J, Chelvarajan RL, Shuck KM, Artiushin S, Timoney PJ, Balasuriya UB. 2016. Allelic variation in CXCL16 determines CD3⁺ T lymphocyte susceptibility to equine arteritis virus infection and establishment of long-term carrier state in the stallion. *PLoS Genet* 12:e1006467. <https://doi.org/10.1371/journal.pgen.1006467>.
43. Holyoak GR, Little TV, McCollum WH, Timoney PJ. 1993. Relationship between onset of puberty and establishment of persistent infection with equine arteritis virus in the experimentally infected colt. *J Comp Pathol* 109:29–46. [https://doi.org/10.1016/S0021-9975\(08\)80238-1](https://doi.org/10.1016/S0021-9975(08)80238-1).
44. Danilenko DM, Rossitto PV, Van der Vieren M, Le Trong H, McDonough SP, Affolter VK, Moore PF. 1995. A novel canine leukointegrin, alpha d beta 2, is expressed by specific macrophage subpopulations in tissue and a minor CD8⁺ lymphocyte subpopulation in peripheral blood. *J Immunol* 155:35–44.
45. Moore PF, Rossitto PV, Danilenko DM. 1990. Canine leukocyte integrins: characterization of a CD18 homologue. *Tissue Antigens* 36:211–220. <https://doi.org/10.1111/j.1399-0039.1990.tb01831.x>.
46. Danilenko DM, Moore PF, Rossitto PV. 1992. Canine leukocyte cell adhesion molecules (LeuCAMs): characterization of the CD11/CD18 family. *Tissue Antigens* 40:13–21. <https://doi.org/10.1111/j.1399-0039.1992.tb01952.x>.
47. Ito D, Imai Y, Ohsawa K, Nakajima K, Fukuuchi Y, Kohsaka S. 1998. Microglia-specific localisation of a novel calcium binding protein, Iba1. *Brain Res Mol Brain Res* 57:1–9. [https://doi.org/10.1016/S0169-328X\(98\)00040-0](https://doi.org/10.1016/S0169-328X(98)00040-0).
48. Ahmed Z, Shaw G, Sharma VP, Yang C, McGowan E, Dickson DW. 2007. Actin-binding proteins coronin-1a and IBA-1 are effective microglial markers for immunohistochemistry. *J Histochem Cytochem* 55: 687–700. <https://doi.org/10.1369/jhc.6A7156.2007>.
49. Deininger MH, Meyermann R, Schluessener HJ. 2002. The allograft inflammatory factor-1 family of proteins. *FEBS Lett* 514:115–121. [https://doi.org/10.1016/S0014-5793\(02\)02430-4](https://doi.org/10.1016/S0014-5793(02)02430-4).
50. Nakayama M. 2014. Antigen presentation by MHC-dressed cells. *Front Immunol* 5:672. <https://doi.org/10.3389/fimmu.2014.00672>.
51. Fabrik BO, Dijkstra CD, van den Berg TK. 2005. The macrophage scavenger receptor CD163. *Immunobiology* 210:153–160. <https://doi.org/10.1016/j.imbio.2005.05.010>.
52. Murray PJ, Wynn TA. 2011. Protective and pathogenic functions of macrophage subsets. *Nat Rev Immunol* 11:723–737. <https://doi.org/10.1038/nri3073>.
53. Chavez-Galan L, Ollerros ML, Vesin D, Garcia I. 2015. Much more than M1 and M2 macrophages, there are also CD169⁺ and TCR⁺ macrophages. *Front Immunol* 6:263. <https://doi.org/10.3389/fimmu.2015.00263>.
54. Yamaguchi T, Fushida S, Yamamoto Y, Tsukada T, Kinoshita J, Oyama K, Miyashita T, Tajima H, Ninomiya I, Munese S, Harashima A, Harada S, Yamamoto H, Ohta T. 2016. Tumor-associated macrophages of the M2 phenotype contribute to progression in gastric cancer with peritoneal dissemination. *Gastric Cancer* 19:1052–1065. <https://doi.org/10.1007/s10120-015-0579-8>.
55. Rugtveit J, Scott H, Halstensen TS, Norstein J, Brandtzaeg P. 1996. Expression of the L1 antigen (calprotectin) by tissue macrophages reflects recent recruitment from peripheral blood rather than upregulation of local synthesis: implications for rejection diagnosis in formalin-fixed kidney specimens. *J Pathol* 180:194–199. [https://doi.org/10.1002/\(SICI\)1096-9896\(199610\)180:2<194::AID-PATH628>3.0.CO;2-P](https://doi.org/10.1002/(SICI)1096-9896(199610)180:2<194::AID-PATH628>3.0.CO;2-P).
56. Grosche A, Morton AJ, Polyak MM, Matyjaszek S, Freeman DE. 2008. Detection of calprotectin and its correlation to the accumulation of neutrophils within equine large colon during ischaemia and reperfusion. *Equine Vet J* 40:393–399. <https://doi.org/10.2746/042516408X302500>.
57. Alvarez B, Sanchez C, Bullido R, Marina A, Lunney J, Alonso F, Ezquerro A, Dominguez J. 2000. A porcine cell surface receptor identified by monoclonal antibodies to SWC3 is a member of the signal regulatory protein family and associates with protein-tyrosine phosphatase SHP-1. *Tissue Antigens* 55:342–351. <https://doi.org/10.1034/j.1399-0039.2000.550408.x>.
58. Herrmann-Hoesing LM, Noh SM, Snekvik KR, White SN, Schneider DA, Truscott T, Knowles DP. 2010. Ovine progressive pneumonia virus capsid antigen as found in CD163- and CD172a-positive alveolar macrophages of persistently infected sheep. *Vet Pathol* 47:518–528. <https://doi.org/10.1177/0300985809359605>.
59. Gulbahar MY, Davis WC, Yuksel H, Cabalar M. 2006. Immunohistochemical evaluation of inflammatory infiltrate in the skin and lung of lambs naturally infected with sheeppox virus. *Vet Pathol* 43:67–75. <https://doi.org/10.1354/vp.43-1-67>.
60. Nalubamba KS, Gossner AG, Dalziel RG, Hopkins J. 2007. Differential expression of pattern recognition receptors in sheep tissues and leukocyte subsets. *Vet Immunol Immunopathol* 118:252–262. <https://doi.org/10.1016/j.vetimm.2007.05.018>.
61. van Beek EM, Cochrane F, Barclay AN, van den Berg TK. 2005. Signal regulatory proteins in the immune system. *J Immunol* 175:7781–7787. <https://doi.org/10.4049/jimmunol.175.12.7781>.
62. McNeilly TN, Brown JK, Harkiss G. 2006. Differential expression of cell surface markers by ovine respiratory tract dendritic cells. *J Histochem Cytochem* 54:1021–1030. <https://doi.org/10.1369/jhc.6A6940.2006>.
63. Aerts-Toegaert C, Heirman C, Tuyaerts S, Corthals J, Aerts JL, Bonehill A,

- Thielemans K, Breckpot K. 2007. CD83 expression on dendritic cells and T cells: correlation with effective immune responses. *Eur J Immunol* 37:686–695. <https://doi.org/10.1002/eji.200636535>.
64. Ni K, O'Neill HC. 1997. The role of dendritic cells in T cell activation. *Immunol Cell Biol* 75:223–230. <https://doi.org/10.1038/icb.1997.35>.
65. Bimczok D, Rothkotter HJ. 2006. Lymphocyte migration studies. *Vet Res* 37:325–338. <https://doi.org/10.1051/vetres:2006004>.
66. Di Carlo E, Magnasco S, D'Antuono T, Tenaglia R, Sorrentino C. 2007. The prostate-associated lymphoid tissue (PALT) is linked to the expression of homing chemokines CXCL13 and CCL21. *Prostate* 67:1070–1080. <https://doi.org/10.1002/pros.20604>.
67. Fritz FJ, Westermann J, Pabst R. 1989. The mucosa of the male genital tract; part of the common mucosal secretory immune system? *Eur J Immunol* 19:475–479. <https://doi.org/10.1002/eji.1830190310>.
68. Fu H, Ward EJ, Marelli-Berg FM. 2016. Mechanisms of T cell organotropism. *Cell Mol Life Sci* 73:3009–3033. <https://doi.org/10.1007/s00018-016-2211-4>.
69. Nguyen PV, Kafka JK, Ferreira VH, Roth K, Kaushic C. 2014. Innate and adaptive immune responses in male and female reproductive tracts in homeostasis and following HIV infection. *Cell Mol Immunol* 11:410–427. <https://doi.org/10.1038/cmi.2014.41>.
70. Zaneveld LJD, Anderson DJ, Whaley KJ, Quayle AJ. 1996. Appendix D, barrier methods and mucosal immunologic approaches, p 430–473. In Harrison PF, Rosenfield A (ed), *Contraceptive research and development: looking to the future*. National Academies Press, Washington, DC.
71. Vairo S, Van den Broeck W, Favoreel H, Scagliarini A, Nauwynck H. 2013. Development and use of a polarized equine upper respiratory tract mucosal explant system to study the early phase of pathogenesis of a European strain of equine arteritis virus. *Vet Res* 44:22. <https://doi.org/10.1186/1297-9716-44-22>.
72. Carossino M, Loynachan AT, James MacLachlan N, Drew C, Shuck KM, Timoney PJ, Del Piero F, Balasuriya UB. 2016. Detection of equine arteritis virus by two chromogenic RNA in situ hybridization assays (conventional and RNAscope (®)) and assessment of their performance in tissues from aborted equine fetuses. *Arch Virol* 161:3125–3136. <https://doi.org/10.1007/s00705-016-3014-5>.
73. Del Piero F, Wilkins PA, Lopez JW, Glaser AL, Dubovi EJ, Schlafer DH, Lein DH. 1997. Equine viral arteritis in newborn foals: clinical, pathological, serological, microbiological and immunohistochemical observations. *Equine Vet J* 29:178–185. <https://doi.org/10.1111/j.2042-3306.1997.tb01666.x>.
74. Cecere TE, Todd SM, Leroith T. 2012. Regulatory T cells in arterivirus and coronavirus infections: do they protect against disease or enhance it? *Viruses* 4:833–846. <https://doi.org/10.3390/v4050833>.
75. Veiga-Parga T, Sehrawat S, Rouse BT. 2013. Role of regulatory T cells during virus infection. *Immunol Rev* 255:182–196. <https://doi.org/10.1111/imr.12085>.
76. Wongyanin P, Buranapraditkul S, Yoo D, Thanawongnuwech R, Roth JA, Suradhat S. 2012. Role of porcine reproductive and respiratory syndrome virus nucleocapsid protein in induction of interleukin-10 and regulatory T-lymphocytes (Treg). *J Gen Virol* 93:1236–1246. <https://doi.org/10.1099/vir.0.040287-0>.
77. Silva-Campa E, Mata-Haro V, Mateu E, Hernandez J. 2012. Porcine reproductive and respiratory syndrome virus induces CD4⁺ CD8⁺ CD25⁺ Foxp3⁺ regulatory T cells (Tregs). *Virology* 430:73–80. <https://doi.org/10.1016/j.virol.2012.04.009>.
78. Cecere TE, Meng XJ, Pelzer K, Todd SM, Beach NM, Ni YY, Leroith T. 2012. Co-infection of porcine dendritic cells with porcine circovirus type 2a (PCV2a) and genotype II porcine reproductive and respiratory syndrome virus (PRRSV) induces CD4⁺ CD25⁺ FoxP3⁺ T cells in vitro. *Vet Microbiol* 160:233–239. <https://doi.org/10.1016/j.vetmic.2012.04.040>.
79. Gomez-Laguna J, Rodriguez-Gomez IM, Barranco I, Pallares FJ, Salguero FJ, Carrasco L. 2012. Enhanced expression of TGFβ protein in lymphoid organs and lung, but not in serum, of pigs infected with a European field isolate of porcine reproductive and respiratory syndrome virus. *Vet Microbiol* 158:187–193. <https://doi.org/10.1016/j.vetmic.2012.02.003>.
80. Kahan SM, Wherry EJ, Zajac AJ. 2015. T cell exhaustion during persistent viral infections. *Virology* 479–480:180–193. <https://doi.org/10.1016/j.virol.2014.12.033>.
81. Wherry EJ, Kurachi M. 2015. Molecular and cellular insights into T cell exhaustion. *Nat Rev Immunol* 15:486–499. <https://doi.org/10.1038/nri3862>.
82. Zuniga EI, Macal M, Lewis GM, Harker JA. 2015. Innate and adaptive immune regulation during chronic viral infections. *Annu Rev Virol* 2:573–597. <https://doi.org/10.1146/annurev-virology-100114-055226>.
83. Wherry EJ. 2011. T cell exhaustion. *Nat Immunol* 12:492–499.
84. Klenerman P, Hill A. 2005. T cells and viral persistence: lessons from diverse infections. *Nat Immunol* 6:873–879. <https://doi.org/10.1038/nri1241>.
85. Roved J, Westerdahl H, Hasselquist D. 2017. Sex differences in immune responses: hormonal effects, antagonistic selection, and evolutionary consequences. *Horm Behav* 88:95–105. <https://doi.org/10.1016/j.yhbeh.2016.11.017>.
86. Miszczak F, Shuck KM, Lu Z, Go YY, Zhang J, Sells S, Vabret A, Pronost S, Fortier G, Timoney PJ, Balasuriya UB. 2011. Evaluation of two magnetic-bead-based viral nucleic acid purification kits and three real-time reverse transcription-PCR reagent systems in two TaqMan assays for equine arteritis virus detection in semen. *J Clin Microbiol* 49:3694–3696. <https://doi.org/10.1128/JCM.01187-11>.
87. Carossino M, Lee PA, Nam B, Skillman A, Shuck KM, Timoney PJ, Tsai Y, Ma L, Chang HG, Wang HT, Balasuriya UB. 2016. Development and evaluation of a reverse transcription-insulated isothermal polymerase chain reaction (RT-iiPCR) assay for detection of equine arteritis virus in equine semen and tissue samples using the POCkit system. *J Virol Methods* 234:7–15. <https://doi.org/10.1016/j.jviromet.2016.02.015>.
88. Pacheco JM, Smoliga GR, O'Donnell V, Brito BP, Stenfeldt C, Rodriguez LL, Arzt J. 2015. Persistent foot-and-mouth disease virus infection in the nasopharynx of cattle; tissue-specific distribution and local cytokine expression. *PLoS One* 10:e0125698. <https://doi.org/10.1371/journal.pone.0125698>.
89. Stenfeldt C, Eschbaumer M, Rekant SI, Pacheco JM, Smoliga GR, Hartwig EJ, Rodriguez LL, Arzt J. 2016. The foot-and-mouth disease carrier state divergence in cattle. *J Virol* 90:6344–6364. <https://doi.org/10.1128/JVI.00388-16>.
90. Stenfeldt C, Pacheco JM, Smoliga GR, Bishop E, Pauszek SJ, Hartwig EJ, Rodriguez LL, Arzt J. 2016. Detection of foot-and-mouth disease virus RNA and capsid protein in lymphoid tissues of convalescent pigs does not indicate existence of a carrier state. *Transbound Emerg Dis* 63:152–164. <https://doi.org/10.1111/tbed.12235>.
91. Prabhudas M, Bowdish D, Drickamer K, Febbraio M, Herz J, Kobzik L, Krieger M, Loike J, Means TK, Moestrup SK, Post S, Sawamura T, Silverstein S, Wang XY, El Khoury J. 2014. Standardizing scavenger receptor nomenclature. *J Immunol* 192:1997–2006. <https://doi.org/10.4049/jimmunol.1490003>.
92. Sarkar S, Chelvarajan L, Go YY, Cook F, Artiushin S, Mondal S, Anderson K, Eberth J, Timoney PJ, Kalbfleisch TS, Bailey E, Balasuriya UB. 2016. Equine arteritis virus uses equine CXCL16 as an entry receptor. *J Virol* 90:3366–3384. <https://doi.org/10.1128/JVI.02455-15>.
93. Izquierdo MC, Martin-Cleary C, Fernandez-Fernandez B, Elewa U, Sanchez-Nino MD, Carrero JJ, Ortiz A. 2014. CXCL16 in kidney and cardiovascular injury. *Cytokine Growth Factor Rev* 25:317–325. <https://doi.org/10.1016/j.cytogfr.2014.04.002>.
94. Morgan AJ, Guillen C, Symon FA, Huynh TT, Berry MA, Entwisle JJ, Briskin M, Pavord ID, Wardlaw AJ. 2005. Expression of CXCR6 and its ligand CXCL16 in the lung in health and disease. *Clin Exp Allergy* 35:1572–1580. <https://doi.org/10.1111/j.1365-2222.2005.02383.x>.
95. Richardsen E, Ness N, Melbo-Jorgensen C, Johannesen C, Grindstad T, Nordbakken C, Al-Saad S, Andersen S, Donnem T, Nordby Y, Bremnes RM, Busund LT. 2015. The prognostic significance of CXCL16 and its receptor C-X-C chemokine receptor 6 in prostate cancer. *Am J Pathol* 185:2722–2730. <https://doi.org/10.1016/j.ajpath.2015.06.013>.
96. Shashkin P, Simpson D, Mishin V, Chesnutt B, Ley K. 2003. Expression of CXCL16 in human T cells. *Arterioscler Thromb Vasc Biol* 23:148–149. <https://doi.org/10.1161/01.ATV.0000043906.61088.4B>.
97. Nakayama T, Hieshima K, Izawa D, Tatsumi Y, Kanamaru A, Yoshie O. 2003. Cutting edge: profile of chemokine receptor expression on human plasma cells accounts for their efficient recruitment to target tissues. *J Immunol* 170:1136–1140. <https://doi.org/10.4049/jimmunol.170.3.1136>.
98. Gunther C, Carballido-Perrig N, Kaesler S, Carballido JM, Biedermann T. 2012. CXCL16 and CXCR6 are upregulated in psoriasis and mediate cutaneous recruitment of human CD8⁺ T cells. *J Invest Dermatol* 132:626–634. <https://doi.org/10.1038/jid.2011.371>.
99. van der Voort R, van Lieshout AW, Toonen LW, Sloetjes AW, van den Berg WB, Figdor CG, Radstake TR, Adema GJ. 2005. Elevated CXCL16 expression by synovial macrophages recruits memory T cells into

- rheumatoid joints. *Arthritis Rheum* 52:1381–1391. <https://doi.org/10.1002/art.21004>.
100. Hedges JF, Demaula CD, Moore BD, McLaughlin BE, Simon SJ, MacLachlan NJ. 2001. Characterization of equine E-selectin. *Immunology* 103:498–504. <https://doi.org/10.1046/j.1365-2567.2001.01262.x>.
 101. Timoney PJ, McCollum WH, Roberts AW, McDonald MJ. 1987. Status of equine viral arteritis in Kentucky, 1985. *J Am Vet Med Assoc* 191:36–39.
 102. World Organisation for Animal Health (OIE). 2016. Equine viral arteritis, chapter 2.5.10. In OIE Biological Standards Commission (ed), *Manual of diagnostic tests and vaccines for terrestrial animals*, 7th ed, vol 2. OIE, Paris, France.
 103. Campos JR, Breheny P, Araujo RR, Troedsson MH, Squires EL, Timoney PJ, Balasuriya UB. 2014. Semen quality of stallions challenged with the Kentucky 84 strain of equine arteritis virus. *Theriogenology* 82: 1068–1079. <https://doi.org/10.1016/j.theriogenology.2014.07.004>.
 104. Balasuriya UB, Leutenegger CM, Topol JB, McCollum WH, Timoney PJ, MacLachlan NJ. 2002. Detection of equine arteritis virus by real-time TaqMan reverse transcription-PCR assay. *J Virol Methods* 101:21–28. [https://doi.org/10.1016/S0166-0934\(01\)00416-5](https://doi.org/10.1016/S0166-0934(01)00416-5).
 105. Heidner HW, Rossitto PV, MacLachlan NJ. 1990. Identification of four distinct neutralizing epitopes on bluetongue virus serotype 10 using neutralizing monoclonal antibodies and neutralization-escape variants. *Virology* 176:658–661. [https://doi.org/10.1016/0042-6822\(90\)90041-O](https://doi.org/10.1016/0042-6822(90)90041-O).
 106. Jensen EC. 2013. Quantitative analysis of histological staining and fluorescence using ImageJ. *Anat Rec (Hoboken)* 296:378–381. <https://doi.org/10.1002/ar.22641>.
 107. Landini G. 2015. Colour deconvolution. School of Dentistry, University of Birmingham, Birmingham, United Kingdom. <http://www.mecourse.com/landinig/software/cdeconv/cdeconv.html>.
 108. Gown AM, Goldstein LC, Barry TS, Kussick SJ, Kandalaf PL, Kim PM, Tse CC. 2008. High concordance between immunohistochemistry and fluorescence in situ hybridization testing for HER2 status in breast cancer requires a normalized IHC scoring system. *Mod Pathol* 21:1271–1277. <https://doi.org/10.1038/modpathol.2008.83>.
 109. Tumas DB, Brassfield AL, Travenor AS, Hines MT, Davis WC, McGuire TC. 1994. Monoclonal antibodies to the equine CD2 T lymphocyte marker, to a pan-granulocyte/monocyte marker and to a unique pan-B lymphocyte marker. *Immunobiology* 192:48–64. [https://doi.org/10.1016/S0171-2985\(11\)80407-9](https://doi.org/10.1016/S0171-2985(11)80407-9).
 110. Liu C, Cook FR, Cook SJ, Craigo JK, Even DL, Issel CJ, Montelaro RC, Horohov DW. 2012. The determination of in vivo envelope-specific cell-mediated immune responses in equine infectious anemia virus-infected ponies. *Vet Immunol Immunopathol* 148:302–310. <https://doi.org/10.1016/j.vetimm.2012.06.018>.
 111. Blanchard-Channell M, Moore PF, Stott JL. 1994. Characterization of monoclonal antibodies specific for equine homologues of CD3 and CD5. *Immunology* 82:548–554.
 112. Lunn DP, Holmes MA, Duffus WP. 1991. Three monoclonal antibodies identifying antigens on all equine T lymphocytes, and two mutually exclusive T-lymphocyte subsets. *Immunology* 74:251–257.
 113. Crump AL, Davis W, Antczak DF. 1988. A monoclonal antibody identifying a T-cell marker in the horse. *Anim Genet* 19:349–357.
 114. Boliar S, Chambers TM. 2010. A new strategy of immune evasion by influenza A virus: inhibition of monocyte differentiation into dendritic cells. *Vet Immunol Immunopathol* 136:201–210. <https://doi.org/10.1016/j.vetimm.2010.03.004>.
 115. Yamate J, Yoshida H, Tsukamoto Y, Ide M, Kuwamura M, Ohashi F, Miyamoto T, Kotani T, Sakuma S, Takeya M. 2000. Distribution of cells immunopositive for AM-3K, a novel monoclonal antibody recognizing human macrophages, in normal and diseased tissues of dogs, cats, horses, cattle, pigs, and rabbits. *Vet Pathol* 37:168–176. <https://doi.org/10.1354/vp.37-2-168>.
 116. Tomokiyo R, Jinnouchi K, Honda M, Wada Y, Hanada N, Hiraoka T, Suzuki H, Kodama T, Takahashi K, Takeya M. 2002. Production, characterization, and interspecies reactivities of monoclonal antibodies against human class A macrophage scavenger receptors. *Atherosclerosis* 161:123–132. [https://doi.org/10.1016/S0021-9150\(01\)00624-4](https://doi.org/10.1016/S0021-9150(01)00624-4).
 117. Merant C, Bonnefont C, Desbos A, Greenland T, Cadore JL, Monier JC. 2003. Cross-species reactivity of seven monoclonal antibodies with equine lymphocytes by flow cytometry. *Vet Res* 34:791–801. <https://doi.org/10.1051/vetres:2003033>.
 118. Hirayama K, Honda Y, Sako T, Okamoto M, Tsunoda N, Tagami M, Taniyama H. 2003. Invasive ductal carcinoma of the mammary gland in a mare. *Vet Pathol* 40:86–91. <https://doi.org/10.1354/vp.40-1-86>.
 119. Bohn W, Wiegers W, Beuttenmuller M, Traub P. 1992. Species-specific recognition patterns of monoclonal antibodies directed against vimentin. *Exp Cell Res* 201:1–7. [https://doi.org/10.1016/0014-4827\(92\)90341-5](https://doi.org/10.1016/0014-4827(92)90341-5).